THESIS

SEDIMENTOLOGY, FACIES ARCHITECTURE AND SEQUENCE STRATIGRAPHY OF THE LOWER BAKKEN SHALE MEMBER IN THE WILLISTON BASIN, NORTH DAKOTA, UNITED STATES OF AMERICA

Submitted by

Stacie Albert

Department of Geosciences

In partial fulfillment of the requirements

For the Degree of Master of Science

Colorado State University

Fort Collins, Colorado

Summer 2014

Master's Committee:

Advisor: Sven O. Egenhoff

Ellen E. Wohl
Gamze Çavdar

ABSTRACT

SEDIMENTOLOGY, FACIES ARCHITECTURE AND SEQUENCE STRATIGRAPHY OF THE LOWER BAKKEN SHALE MEMBER IN THE WILLISTON BASIN, NORTH DAKOTA, UNITED STATES OF AMERICA

The Upper Devonian lower shale member of the Bakken Formation in the North Dakota portion of the Williston Basin consists predominantly of organic-rich (up to 20 wt % total organic carbon (TOC)), black siliciclastic mudstones and displays a total gamma ray (GR) log profile that commonly ranges between 200 and 900 API units. Eleven fine-grained facies, ten siliciclastic and one carbonate, are identified in the succession based on sedimentological characteristics and grouped into four distinct facies associations (FAs). FA 1 is characterized by the presence of pure radiolarites and also contains massive mudstones and abundant radiolaria-bearing mudstones. Laminated mudstones of FA 2 consist predominantly of partially- to well-laminated silt-bearing mudstones with foresets of alternating siltstone and mud-rich laminae in places. Deposits of FA 3, bioturbated mudstones with macrofossil debris, are dominated by phosphate- and fossil-debris bearing mudstones. The silt-rich mudstones of FA 4 are composed primarily of continuous and discontinuous siltstone laminae.

The lower Bakken shale member is subdivided into four stratigraphic units termed Interval 1-4. Interval 1 is located at the bottom of the succession and is dominated by abundant bioturbation, fossil debris and lag deposits. The overlying Interval 2 is characterized by intercalated radiolaria-bearing mudstones with silt-bearing massive to faintly- and well-laminated mudstones. Stratigraphic Interval 3 is located just above Interval 2 and is comprised

mainly of massive mudstones and abundant radiolaria-bearing mudstones that commonly coarsen-upward into siltstone laminae and thin beds near the base of the overlying Interval 4. The uppermost Interval 4 consists of siltstone laminae or lag deposits at its base that generally fine-upward into massive mudstones.

Each of the four FAs recognized in the lower Bakken shale member are interpreted to represent a distinct position along a proximal to distal offshore ramp transect in this mudstone system. FA 4 rocks were deposited in the most proximal setting, as they are characterized by indicators of high-energy conditions in mudstones, such as phosphate and fossil clasts, as well as erosional bases. Basinwards of FA 4, mudstones of FA 3 and FA 2 are slightly finer-grained than the most proximal deposits and reflect an overall decrease in depositional energy. The very-fine grained massive mudstones and local radiolarites of FA 1 record deposition in the most distal and tranquil regions of the basin.

Bedload transport processes were active across all FAs and are indicated by high-energy lenticular siltstone laminae interpreted as caused by events, lag deposits and clay clasts. Suspension settling processes are responsible for depositing some of the lower Bakken shale member facies, such as the radiolarites (facies 1) and sub-mm laminae of clay-rich mudstones (facies 3).

Medium-scale parasequences in the lower Bakken shale member, represented by stratigraphic Intervals 1-4 in this study, can be traced laterally through the basin supporting a sequence stratigraphic interpretation. The lower half of the succession, Intervals 1 and 2, are interpreted to represent deposits of a transgressive systems tract (TST), characterized by massive and radiolaria-mudstones overlying silt-rich mudstones and heavily bioturbated, fossil-bearing mudstones. Interval 3 likely represents deposits of an early highstand systems tract (HST), as

evidenced by rare high-energy event laminae and abundant massive and radiolaria-bearing mudstone laminae. Interval 4 possibly records a late highstand and in places progrades, but, in general, it displays a fining-upward trend that may represent a short-term transgressive pulse.

The presence of *Phycosiphon incertum* fecal strings in all FAs, along with a small number of ichnofossils and shell fragments throughout the succession, indicates that the lower Bakken shale member was likely deposited in dysoxic conditions rather than anoxic conditions as previously suggested.

ACKNOWLEDGEMENTS

It is with immense gratitude that I acknowledge the support, patience and help of my advisor, Dr. Sven Egenhoff. I would sincerely like to thank Marathon Oil Company for financing this research project. I would also like to thank Dr. Sven Egenhoff and Damien Borcovsky for hand logging some of the cores during our trips to the core library in Grand Forks, North Dakota.

I am very grateful for my committee members, Dr. Sven Egenhoff, Dr. Ellen Wohl, and Dr. Gamze Çavdar who provided me with invaluable suggestions and comments. I would also like to thank Heather Lowers and Adam Boehlke from the United States Geological Survey (USGS) for their assistance in obtaining access to SEM and XRD analyses, and also Julie LeFever from the North Dakota Geological Survey for the lower Bakken shale isopach ArcGIS shapefile that was used in several figures throughout this thesis.

I am especially grateful for the amazing students in the sedimentology working group at Colorado State University who were always willing to help and made our office a great place to work. Lastly, I would like to thank my family and Rob Kahl for their continued love, support and encouragement.

TABLE OF CONTENTS

1.0 INTRODUCTION

Organic-rich siliciclastic mudstones, in common use often described as shales, generally show a massive appearance in both outcrop and core (Macquaker and Gawthorpe, 1993; Macquaker and Jones, 2002; Schieber and Southard, 2009). This lack of macroscopically discernible features and the fact that in normal 30 µm-thick thin section very little, if anything, is visible (Schieber and Zimmerle, 1998) has hindered a detailed description of the often miniscule or subtle sedimentary structures that are present in these fine-grained rocks (Abouelresh and Slatt, 2012; Macquaker and Howell, 1999; Macquaker et al. 2010; Schieber, 1998b). Therefore, detailed facies and microfacies descriptions of organic-rich mudstones that would also allow for a sequence stratigraphic interpretation of these fine-grained rocks are still relatively rare in the literature (Bohacs et al., 2002; Hammes and Frébourg, 2012; Macquaker and Taylor, 1996; Macquaker and Jones, 2002; Macquaker et al., 1998, 2007; Schieber, 1998a) despite the growing importance of siliciclastic mudstones in the petroleum industry as unconventional reservoirs (Aplin and Macquaker, 2010). A prime example of such an organic-rich siliciclastic mudstone unit is the lower member of the Upper Devonian Bakken Formation which, together with the middle and the upper Bakken member, is currently one of the most significant exploration targets in the Williston Basin of North Dakota and Montana, USA. The two "shales" marking the top and the bottom of this unit show average TOC values of 8% and 10% and are known to be world-class source rocks that have supplied oil to both stratigraphically over- and underlying units (Chen et al. 2009; Meissner, 1978; Meissner and Banks, 2000; Pollastro et al., 2008; Smith and Bustin, 1998). Whereas, the sedimentology of the upper shale member of the Bakken Formation has been recently described in detail (Borcovsky, 2013; Egenhoff and Fishman,

2013), the considerably thicker and more organic-rich siliciclastic mudstones of the lower shale member have not been given much attention, even though they are likely more significant as both a source rock and unconventional reservoir.

The present study is therefore the first that sheds light on the facies and internal architecture of the lower Bakken shale in the Williston basin of North Dakota. This study illustrates that the lower member, similar to the upper member of the Bakken shale, contains a predictable internal architecture, yet is significantly different from its younger counterpart. Like the upper shale member of the Bakken Formation, the lower member is made up of several parasequences that can be traced over several hundred kilometers laterally, with some of them being time-equivalent to the overlying middle Bakken member. This study therefore shows that sequence stratigraphy is applicable to fine-grained mudstone systems, such as the black shales of the lower member of the Bakken Formation, which allows predicting the occurrence of high total organic carbon (TOC) and potentially fraccable facies stratigraphically as well as aerially on a basin scale.

2.0 GEOLOGICAL SETTING

The Williston Basin is a semicircular intracratonic basin that spans North and South Dakota and Montana in the United States and southern Saskatchewan and Manitoba in Canada (Fig. 1). Slow subsidence began in the Cambrian but became more intense in the Ordovician (Gerhard et al., 1990). The basin fill contains a continuous Phanerozoic rock record; in the center of the basin, this succession can be over 16,000 feet (nearly 5000 meters) thick. As part of the North American craton, the Williston Basin's sedimentation history can be characterized as predominantly carbonate deposition until the mid-Mississippian and transitions largely to clastic deposition through the Cenozoic (Murphy et al., 2009).

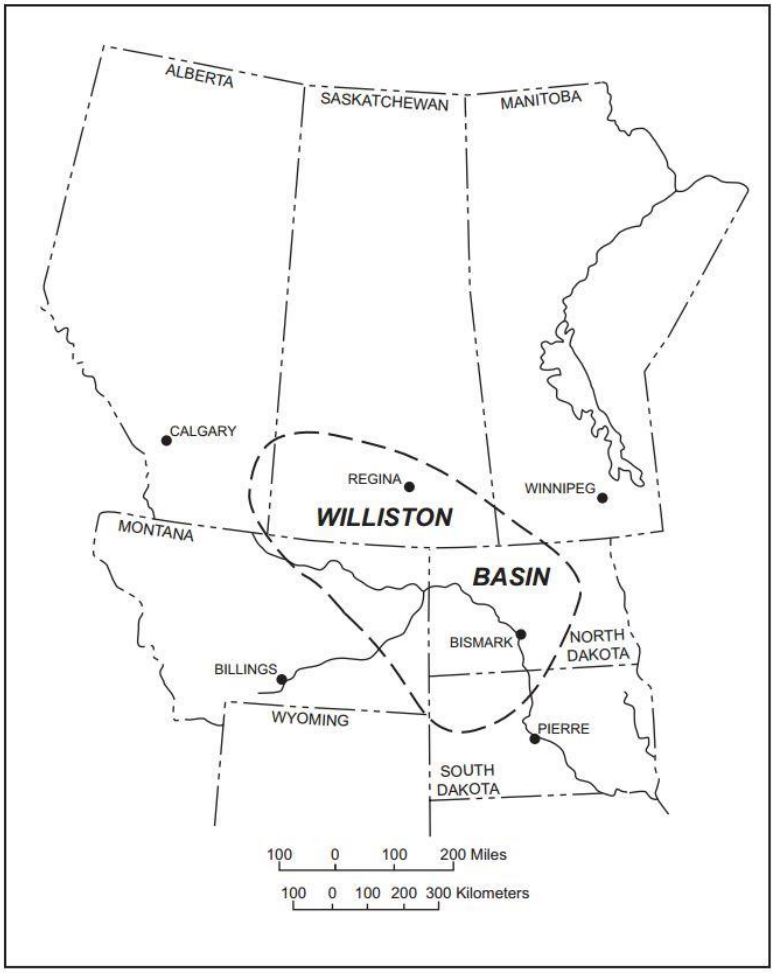

Figure 1 (Previous Page). Map showing approximate extent of the Williston Basin (Pitman et al., 2001).

During Bakken deposition, in the Late Devonian to Early Mississippian, the Williston Basin was positioned approximately 5° to 10° N from the Equator (Ettensohn and Barron, 1981) and was covered by a large epicontinental sea that occupied the western portion of the North American craton (Smith and Bustin, 1998). The climate across most of the ancient continental mass, Laurasia, that included North America at this time was tropical to savannah-like with seasonally wet to dry conditions and generally low rainfall levels (Woodrow et al., 1973). The Williston Basin was partially enclosed while maintaining an opening on the western margin of the North American craton allowing for access to open, deep marine waters (Gerhard and Anderson, 1988) (Fig. 2).

The Bakken Formation is a relatively thin, organic-rich unit present only in the subsurface in the central and deeper portions of the Williston Basin. Stratigraphically, the Bakken Formation is underlain by the Three Forks and overlain by the Lodgepole Formations (Fig. 3) The thickness of the Bakken Formation reaches its maximum of approximately 160 feet (approximately 50 meters) (Pollastro et al., 2011) in northwest North Dakota east of the Nesson Anticline (Sonnenberg and Pramudito, 2009), which is an elevated zone located approximately in the center of the Williston Basin (Laird and Folsom, Jr., 1956). The unit thins to zero close to the basin margin. Traditionally, three members are identified within the Bakken: 1) an organic-rich black mudstone lower member; 2) a mixed carbonate and siliciclastic middle member; and 3) a black mudstone upper member, similar in composition to the lower member (LeFever, 1991; Meissner, 1978; Pollastro et al., 2011; Smith and Bustin, 1995).The lower Bakken member is believed to have formed during an episode of sea level rise in the basin center that was located below the storm-wave base (Smith and Bustin, 1995). After the deposition of the lower member,

the carbonates and siltstones (Schmoker and Hester, 1983) of the middle Bakken member accumulated in a coastal to shallow-marine environment after a drop in sea level (Smith and Bustin, 1995). Following another rise in sea level, the black mudstones of the Upper Bakken Member formed (Smith and Bustin, 1995).

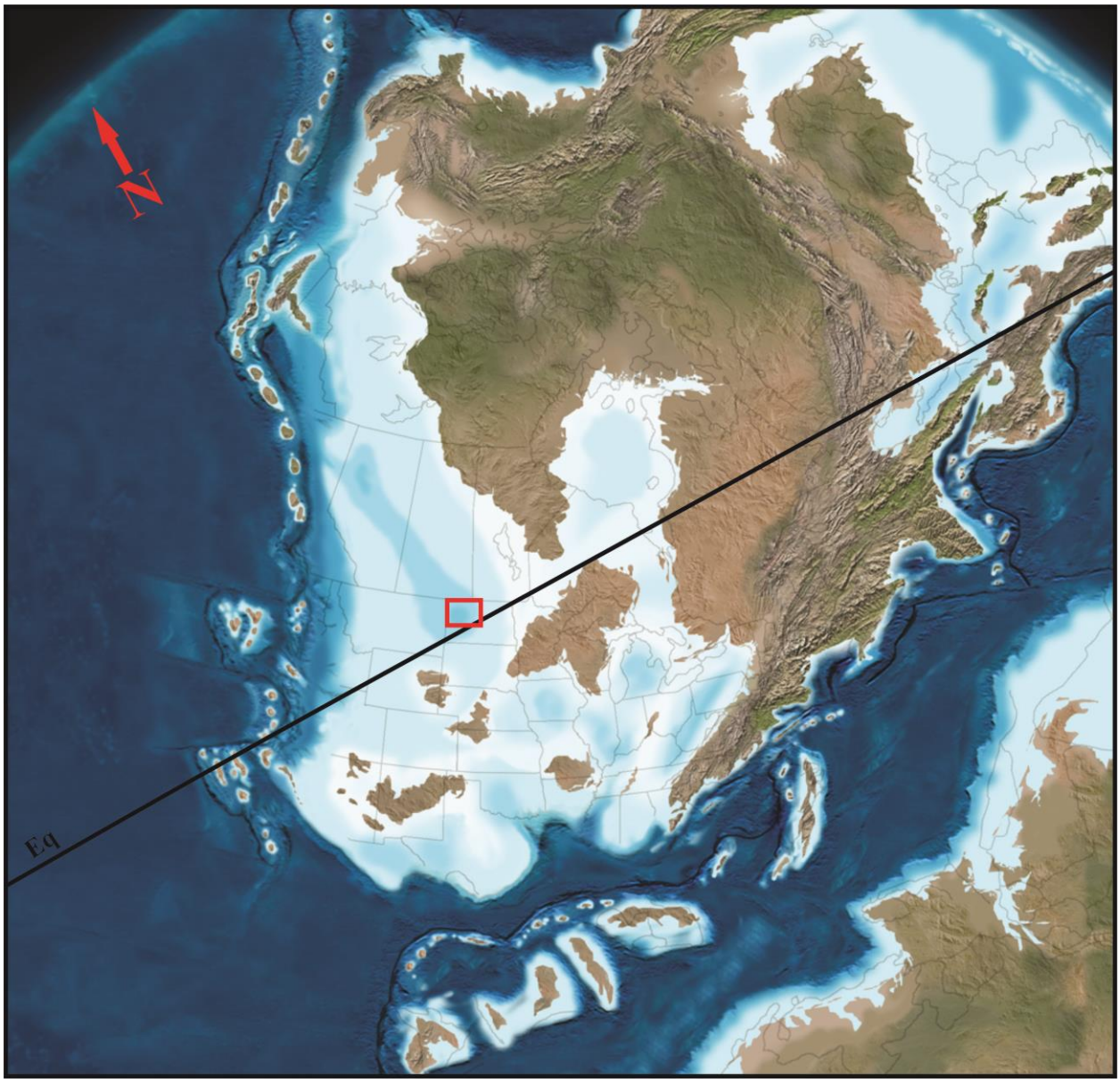

Figure 2. Late Devonian-Early Mississippian (375-345 Ma) paleogeography of North America. Red box indicates approximate location of the study area, northwest North Dakota, and the black line indicates approximate location of the paleoequator (Modified from Ron Blakey, Colorado Plateau Geosystems, Inc., 2012).

The basin is well known for its large hydrocarbon potential in many stratigraphic intervals between the Cambrian and the Triassic. Important reservoirs are of Ordovician and Devonian-Mississippian age (Montgomery, 1997). Estimates for the Devonian-Mississippian Bakken Formation indicate that there are 3.65 billion barrels of recoverable oil in this formation alone within the U.S. portion of the Williston Basin (Pollastro et al., 2008). Although the majority of oil exploration efforts are currently focused on the Middle Bakken Member, the original target within this formation was the Upper Member (Hansen, 1991). The Upper and Lower Shale Members of the Bakken Formation have been identified as the source rocks for the Middle Bakken Member (Hansen, 1991), as well as for various over- and underlying units and are considered to be the most important source rocks in the entire Williston Basin (e.g. Gerhard et al., 1990; Chen et al., 2009).

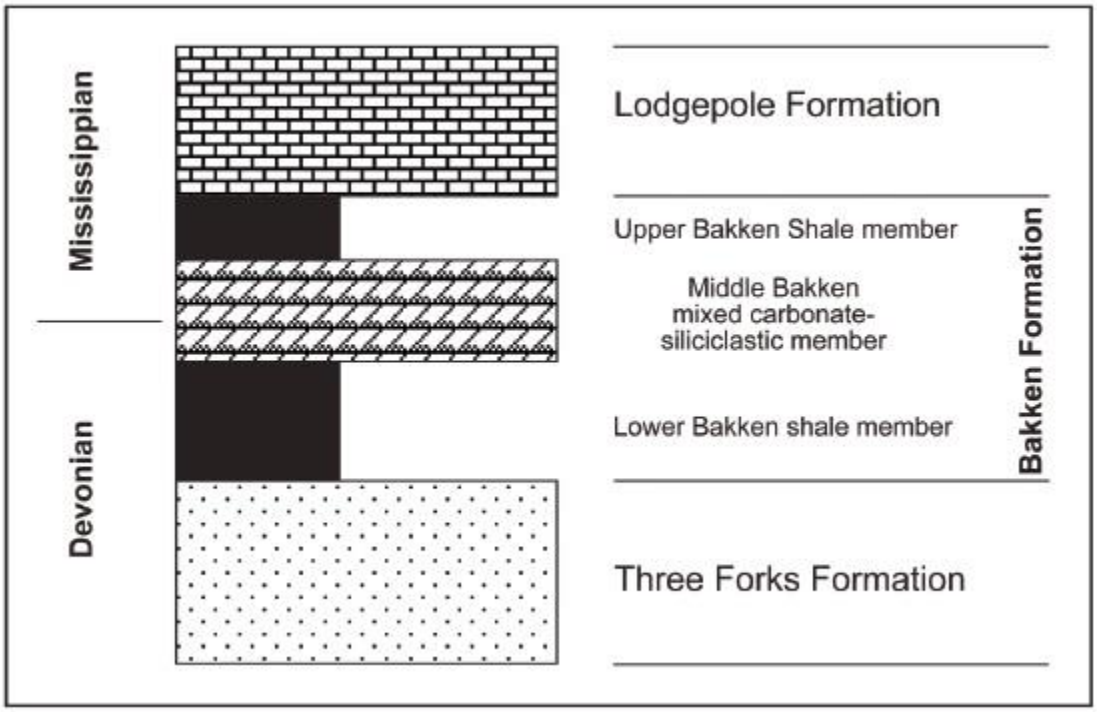

Figure 3. Generalized stratigraphic section of the Bakken Formation and under- and overlying units, and its subdivision into a lower and upper shale member, and a middle mixed carbonate-siliciclastic member (Egenhoff et al., 2011).

3.0 METHODOLOGY

The data on the lower shale member of the Bakken Formation used in this study are from detailed sedimentologic descriptions of drill core made available by the North Dakota Geological Survey (NDGS) Wilson M. Laird Core and Sample Library in Grand Forks, North Dakota (see Appendices 1-4). Cores for observation were selected based on their position in the area of interest to ensure a basin-wide analysis (Table 1; Fig. 4). The drill core sections were hand-drafted on site in North Dakota and focused on recording small-scale (mm-cm) lithological variations in the succession; the sections were later digitized in CorelDraw X6 for further analysis and correlation. Representative samples obtained from the NDGS were taken throughout the stratigraphic interval and labeled with their well number and depth, and marked for accurate stratigraphic orientation.

Samples collected from the drill core were prepared for microscopic analysis at the Colorado State University Sedimentology Laboratory. Before the samples were cut perpendicular to bedding using a traditional rock saw, they were coated with epoxy resin in order to prevent breakage and disintegration. Ultra-thin sections approximately 20 μm in thickness were then prepared from the cut samples by Wagner Petrographic in Lindon, Utah. The thin sections were made to the standard size of 24x46mm, left uncovered and polished. Sedimentological features, such as lithology, bedding thickness, grain size distribution and sedimentary structures, were determined using transmitted light microscopy under a Nikon SMZ1500 stereo petrographic microscope with a magnification range from 0.75x to 11.25x. Scanning electron microscopy (SEM) was used on some ultra-thin sections in order to determine the texture and composition of clay-sized material and organic matter in the matrix. The United

States Geological Survey (USGS) in Denver, Colorado assisted in preparing the ultra-thin sections for analysis by coating the selected samples in carbon and aided in examination by using a Quatra 450 FEG scanning electron microscope equipped with energy-dispersive X-ray spectroscopy (EDS) in backscattered electron (BSE) mode. SEM and EDS technology provide detailed imagery and chemical characterization of a sample, respectively, while BSE detectors are placed above a sample and collect electrons scattered as a function of sample composition (Schieber, 2003).

A total of forty-two samples were examined for total organic carbon content (TOC). Samples were initially treated with hydrochloric acid to remove carbonate materials and TOC analyses were then carried out using standard induction furnace techniques at Weatherford Laboratories in Houston, Texas. These data facilitated the identification of a range of organic carbon values for each lower Shale member facies, as well as the determination of T_{max} and maturity.

X-ray diffraction (XRD) analyses were performed on ten samples at the USGS in Denver, Colorado using the technique developed by Eberl (2003) to provide quantitative whole rock mineralogic data after organic carbon was removed from each powdered sample as summarized by Soukup et al. (2008). This method aided in the identification of clay minerals (see Drever, 1973 and Pollastro, 1982) and determined their amount in the sample.

Table 1. List of wells with cores that were logged in this study. Well localities are shown in Figure 4. The well ID number refers to the North Dakota Geological Survey well file number.

Map Locator #	Original Operator	Original Well Name	Well ID #
1	BRIGHAM OIL & GAS, L.P.	OLSON 10-15 1-H	17513
2	NEWFIELD PRODUCTION COMPANY	CHANEL 1-33H	18226
3	NORTH PLAINS ENERGY, LLC	SCANLAN 3-5H	18770
4	AMERADA HESS CORPORATION	ANDERSON SMITH 1-26H	16083
5	AMERADA HESS CORPORATION	STATE 36-31H	15674
6	HEADINGTON OIL COMPANY, LLC	NESSON STATE 42X-36	17015
7	SHELL OIL COMPANY	L. TEXEL #21-35	5088
8	HESS CORPORATION	RS-NELSON 1423H-1	16824
9	HESS CORPORATION	RS-STATE 3603H-1	17071
10	EOG RESOURCES, INC.	MCALMOND 1-05H	16862
11	HESS CORPORATION	IM-SHORTY 0805H-1	17272
12	GOLDEN EYE RESOURCES	J. BREKHUS #12-14H	17347
13	NEWFIELD PRODUCTION COMPANY	SERGEANT MAJOR 1-21H	18086
14	ORYX ENERGY COMPANY	STENEHJEM HD 27-1	13098
15	AMERADA PETROLEUM CORPORATION	CATHERINE E. PECK #2	1405
16	SUN EXPLORATION & PRODUCTION CO.	SUN MARATHON SHOBE #1	12033
17	MARATHON OIL COMPANY	MYLO WOLDING 14-11	18511
18	EOG RESOURCES, INC.	LIBERTY 2-11H	18101
19	EOG RESOURCES, INC.	FERTILE 1-12H	16743
20	POGO PRODUCING COMPANY, LLC	PEGASUS 2-17H	16405
21	HESS CORPORATION	H. BAKKEN 12-07H	16565
22	BURLINGTON RESOURCES O&G CO., LP	WASHBURN 44-36H	17309
23	AMERADA PETROLEUM CORPORATION	JENS STRAND #1	1202
24	TEXACO INC.	F.P. KEOGH #4	2820
25	NEWFIELD PRODUCTION COMPANY	JORGENSON 1-15H	17086
26	MARATHON OIL COMPANY	CORRINE OLSON 34-20	19118
27	JERRY CHAMBERS	USA #1-24	8251
28	TENNECO OIL COMPANY	MEE USA #3-17	7887
29	HESS CORPORATION	STATE OF ND 1-11H	16160
30	WHITING OIL & GAS CORPORATION	BRAAFLAT 11-11H	17023
31	EOG RESOURCES, INC.	VAN HOOK 1-13H	16997
32	PAN AMERICAN PETROLEUM CORP.	JACOB HUBER #1	2618
33	XTO ENERGY INC.	MILLER 34X-9	17723

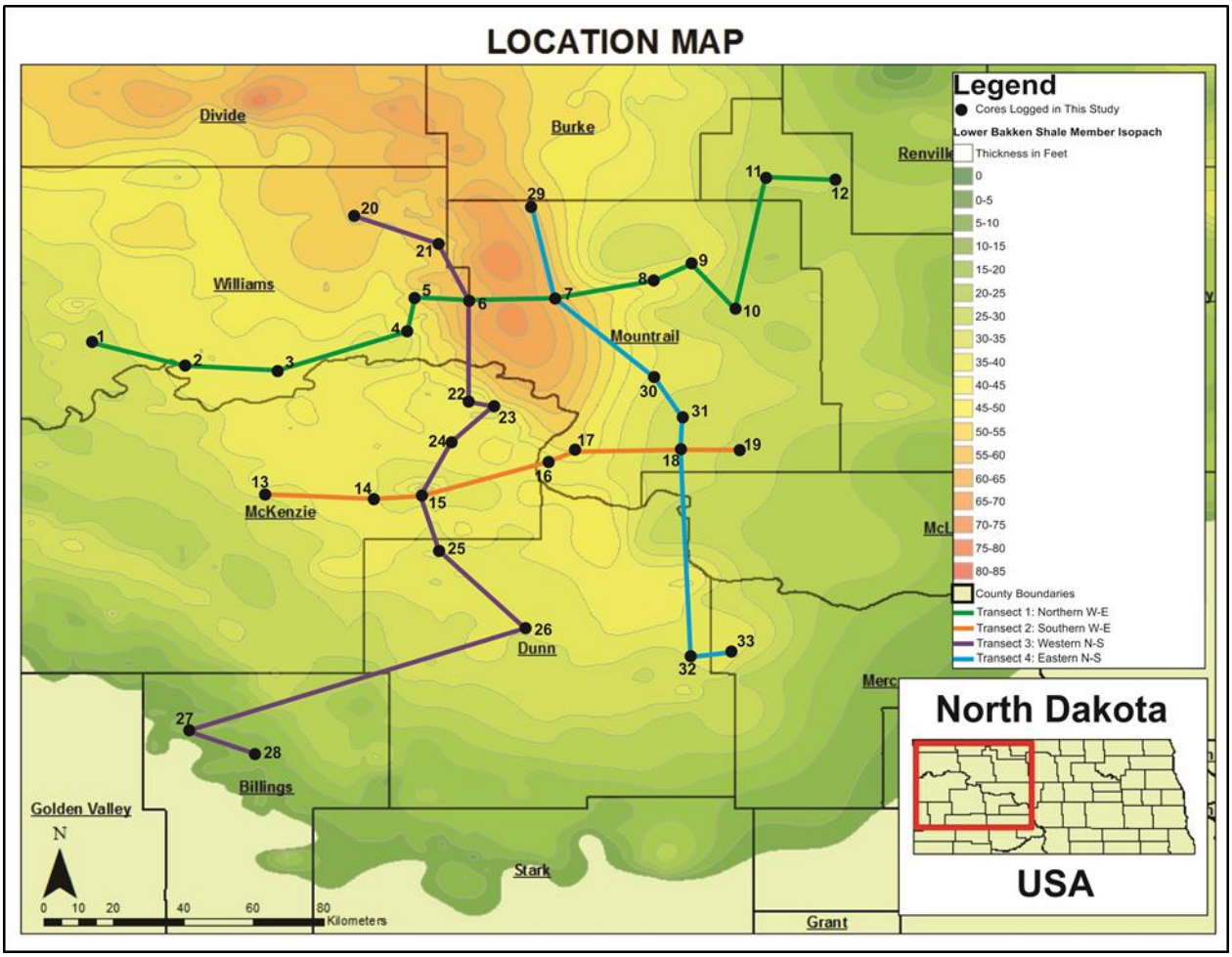

Figure 4. Isopach map of the lower Bakken shale member showing well locations of cores used in this study (Table 1) and transects located in Appendices 1-4. The lower Bakken shale isopach shapefile by J. LeFever (pers. comm., 2012).

4.0 SEDIMENTOLOGY

4.1 Introduction

The sedimentological observations summarized below are based on both the macroscopic and microscopic study of thirty-three cored wells focusing exclusively on the lower Bakken shale member. Illustrated sections of these cores documented at the NDGS in Grand Forks, North Dakota are presented in four transects through the study area in Appendices 1-4. Forty-eight thin sections were described in detail and, along with the documented core descriptions, facilitated the subdivision of the lower Bakken shale member into a total of eleven facies, ten of which are siliciclastic and one of which is a carbonate facies (Table 2; Fig. 5). The subdivision is based on composition, grain size and sedimentary structures, if present; facies nomenclature for this study is slightly modified from the scheme outlined by Macquaker and Adams (2003). The eleven facies recognized in the lower Bakken shale member are grouped into four facies associations (FAs) based on a close co-occurrence within a distinct stratigraphic interval (Table 3). The Lower Bakken Shale FAs are: (FA 1) siliceous black mudstones, (FA 2) laminated mudstones, (FA 3) bioturbated mudstones with macrofossil debris, and (FA 4) silt-rich mudstones (modified from Borcovsky, 2013; Egenhoff and Fishman, 2013). All FAs contain diagenetic calcite, quartz and dolomite minerals and display evidence of bioturbation.

4.2 Burrows

The lower Bakken shale member is characterized by four types of burrows and two types of fecal strings that are common in most of the unit's sediments. *Planolites* burrows and *Phycosiphon* fecal strings occur throughout the entire lower Bakken shale interval. Two forms of the horizontal *Planolites* burrows, herein termed *Planolites* type A and *Planolites* type B,

occur in lower Bakken shale sediments (see Egenhoff and Fishman, 2013, for the upper Bakken shale member): *Planolites* type A burrows are typically 0.3 to 1 mm across and generally less than 1 mm in height, while *Planolites* type B can be up to 10 mm across and as much as 3 mm in height. *Chondrites* and *Teichichnus* burrows occur exclusively in the basal portions of the lower Bakken member. Silt-filled *Chondrites*, similar to those described by Smith and Bustin (2000), are generally preserved as small branching burrows. These burrow types are relatively rare and typically 0.2-12 mm in width. Horizontally-oriented *Teichichnus* burrows are typically stacked in a vertical pattern and appear as U-shaped tongues of sediment (cf. Buatois and Mángano, 2011). They are filled with both carbonate and quartz silt grains and can reach up to 0.5 mm in length.

The two types of fecal strings in the lower Bakken shale interval are (1) *Phycosiphon* isp. fecal strings that occur horizontal to bedding and can be up to 1.5 mm across and as much as 0.3 mm in height, and (2) *Phycosiphon incertum* fecal strings that are ubiquitous and smaller than *Phycosiphon* isp. fecal strings, generally 0.2-0.4 mm across, up to 10 mm long and can occur at any angle to bedding.

4.3 Sedimentary Facies

Table 2. Modified from Borcovsky (2013) and Egenhoff and Fishman (2013)

Facies Name	Facies Thickness	Description and Sedimentary Structures	Composition	Interpretation
Radiolarite **(Facies 1)**	1-10 mm	• Structureless laminae with even geometry • Facies rare throughout succession	• 70-90% radiolaria tests • 15-30% clay-rich matrix with up to 5% amorphous organic matter (AOM)	• Suspension sedimentation of radiolaria tests during blooms • Absence of burrows and fecal strings likely suggests anoxic bottom water conditions
Radiolaria-bearing mudstone **(Facies 2)**	1-50 mm	• Planar to wavy continuous and discontinuous layers, typically with sharp upper and basal contacts • Fabric massive to laminated; compacted fractures filled with pyrite, quartz and calcite common • In places, ripple structures are preserved • Varying abundances of *Phycosiphon incertum* fecal strings	• 45-70% dark brown to black clay-rich matrix with AOM • 15-55% radiolaria tests • 2-15% detrital and siliciclastic silt grains • 1-5% *Tasmanites* algae	• Mixing of radiolaria tests with silt-poor, clay-rich sediment by bedload processes • Ripples indicate reworking by bottom currents • Bioturbation by *Phycosiphon incertum* fecal strings likely produced the massive fabric • Low diversity of ichnofossils indicates dysoxic bottom waters
Massive, clay-rich mudstone **(Facies 3)**	0.1-1 mm	• Continuous, massive laminae of clay-dominated mudstone • Variable abundance of *Phycosiphon incertum* fecal strings	• 80-99% dark brown to black clay-rich matrix with AOM • 1-20% fine- to coarse-silt size siliciclastic and carbonate grains	• Suspension settling of clay and silt-sized detrital grains and AOM in a quiet setting • Low diversity of ichnofossils suggests bottom waters were likely dysoxic
Silt-bearing mudstone **(Facies 4a)**	1-1000 mm	• Predominantly massive in texture, individual laminae can be normally graded in places • Planar laminae and relict laminae 0.5-3 mm thick, in places lateral changes in thickness • Pyrite concretions 0.1-150 mm in length (ave. 0.1-10 mm); pyrite lenses and discontinuous pyrite laminae common • Moderately to highly bioturbated by *Phycosiphon incertum* fecal strings and *Planolites* type A burrows	• 65-90% clay-rich matrix with AOM • 10-35% detrital siliciclastic and carbonate silt (ave. 27%) • 0-10% *Tasmanites* algae • 0-2% silt-size phosphate and fossil clasts	• Depositional process unclear due to intense bioturbation that destroyed the original sedimentary fabric; however, lateral thickness changes of laminae imply bedload transport • Normal grading of laminae suggests deposition from waning flow • Low diversity of ichnofossils suggests bottom waters were most likely dysoxic
Silt- and clay-clast-bearing mudstone **(Facies 4b)**	0.5-25 mm	• Planar, massive and normally-graded laminae 0.5-2 mm thick; laminasets can be up to 25 mm thick • Abundant flaser-shaped clay clasts typically 0.01-0.3 mm in length and 0.02-0.04 mm in thickness • Weakly to moderately bioturbated by *Phycosiphon incertum* fecal strings and rare *Planolites* type A burrows	• 20-60% clay-rich matrix with AOM • 15-25% clay clasts • 8-25% detrital siliciclastic and carbonate silt • 0-10% *Tasmanites* algae • 0-5% silt-size phosphate and fossil clasts	• Bedload transport processes dominated deposition as supported by abundance of clay clasts • Abundance of clay clasts implies up-dip source of clay-rich sediment (Schieber et al., 2010) • Low diversity of ichnofossils indicates dysoxic bottom waters

Tasmanites-bearing mudstone **(Facies 5)**	1- >20mm	• Laterally continuous *Tasmanites*-bearing massive to partially- or well-laminated mudstone • *Tasmanites* algae 0.05-2 mm in length; mostly thick-walled variety • *Tasmanites* algae typically flattened but can be infilled with quartz • Very rare agglutinated foraminifera 0.1-0.25 mm in length • Weakly to moderately bioturbated by *Phycosiphon incertum* fecal strings	• 50-90% dark brown organic matter-bearing clay matrix • 10-50% *Tasmanites* algae (ave. 25%) • 0-5% phosphate and fossil clasts	• Deposition likely by suspension processes as evidenced by constant lateral thickness of laminae, however, bioturbation has disrupted some of the original fabric • Moderate ichnofossil diversity suggests bottom waters were probably dysoxic to oxic
Mudstone with downlapping laminae **(Facies 6)**	1-5 mm	• Low-angle downlapping and converging silt-bearing clay-rich laminae • Alternating silt-rich and mud-rich laminae in places • Weakly to moderately bioturbated by *Phycosiphon incertum* fecal strings	• 60-85% clay-rich matrix with AOM • 15-40% silt-size detrital siliciclastic and carbonate grains	• Downlapping laminae represent ripple foresets formed by bottom currents • Dysoxic bottom waters likely as indicated by low diversity of ichnofossils
Phosphate- and fossil-bearing mudstone **(Facies 7a)**	0.1-15 mm	• Massive laminae and thin beds with even and undulating geometries • Lenses and rare basal scour surfaces in places • Fossil clasts predominantly whole and fragmented conodonts, crinoids and sponge fragments • Disseminated radiolaria tests occur with fossil clasts • Varying abundances of *Phycosiphon* isp., *Phycosiphon incertum* and *Planolites* type A and type B	• 15-60% clay-rich matrix with AOM • 10-50% phosphate and fossil clasts • 25-30% silt-size detrital siliciclastic and carbonate grains • 5-15% silt-size pyrite • 0-10% *Tasmanites* algae • 0-5% sand-size detritus	• Lags deposited during high energy events, as indicated by the abundance of phosphate, pyrite and fossil fragments • Moderate ichnofossil diversity suggests dysoxic to oxic bottom waters
Clay-clast-, phosphate- and fossil-bearing mudstone **(Facies 7b)**	0.1-10 mm	• Massive laminae and thin beds • Lenses and rare basal scour surfaces in places • Frequent flaser-shaped clay clasts generally 0.02-0.3 mm in length and 0.01-0.04 mm in height • Fossil clasts mostly whole and fragmented conodonts, crinoids and sponge pieces • Radiolaria tests occur with fossil clasts • Varying abundances of *Phycosiphon* isp., *Phycosiphon incertum* and *Planolites* type A and type B	• 10-50% dark brown clay-rich matrix with AOM • 15-45% clay clasts • 10-40% phosphate and fossil clasts • 8-25% detrital siliciclastic and carbonate silt • 2-15% silt-size pyrite • 0-10% *Tasmanites* algae • 0-5% sand-size detritus	• Lags deposited during high energy events • Clay clasts derived from up-dip erosion of clay-rich sea floor sediments and redeposited by bedload processes (Schieber et al., 2010) • Moderate ichnofossil diversity suggests dysoxic to oxic bottom waters
Macrofossil-bearing mudstone **(Facies 8)**	10-400 mm	• Whole and fragmented shells 1-20 mm in length • Varies from intensely bioturbated with no visible structures to faintly laminated • *Planolites* type A and type B burrows, *Phycosiphon incertum* fecal strings	• 30-85% dark brown clay-rich matrix with AOM • 15-30% silt-size detrital siliciclastic and carbonate grains • 2-8% shells	• Fragmented shells likely imply transport by bedload processes, however, bioturbation destroyed much of the original fabric • Dysoxic to oxic bottom waters indicated by bioturbation from benthic organisms and abundance of autochthonous fossil debris

Macrobioturbated mudstone **(Facies 9)**	5-75 mm	• Bioturbated fabric with rare relict silt-bearing to silt-rich laminae • Highly bioturbated by *Planolites* type A and type B burrows and *Phycosiphon incertum* fecal strings • Rare *Chondrites* and *Teichichnus* burrows	• 35-85% medium to dark brown clay-rich matrix with AOM • 15-35% siliciclastic and carbonate silt	• Depositional process unclear due to bioturbation • Moderate diversity of ichnofossils suggests dysoxic to oxic bottom waters
Siltstone **(Facies 10)**	0.5-50 mm	• Typically individual laminae 0.5-1 mm thick that display even and/or undulating geometries • Laminasets can be up to 50 mm in places • Preserved ripples structures • *Phycosiphon incertum* fecal strings are common • Silt-filled *Planolites* type B burrows are rare	• 85-99% detrital carbonate and siliciclastic silt • 1-15% dark brown clay-rich matrix • 0-5% fine sand-size siliciclastic detritus	• Sporadic, high-energy events transported and deposited irregular silt laminae by bedload processes • Distal tempestites • Ripple structures occur in places and indicate deposition by bedload transport • Low diversity of ichnofossils suggests dysoxic bottom waters
Skeletal packstone **(Facies 11)**	5-20 mm	• Skeletal clasts mostly fine- to medium-sand size, but some fragmented sponge pieces up to 9mm in length • Basal erosion surfaces	• 55% skeletal clasts • 45% micrite	• Deposition of carbonate lag by bottom currents likely sourced from the paleoshoreline • Sub-parallel arrangement of clasts to bedding suggests reworking during or after deposition in a relatively high energy environment

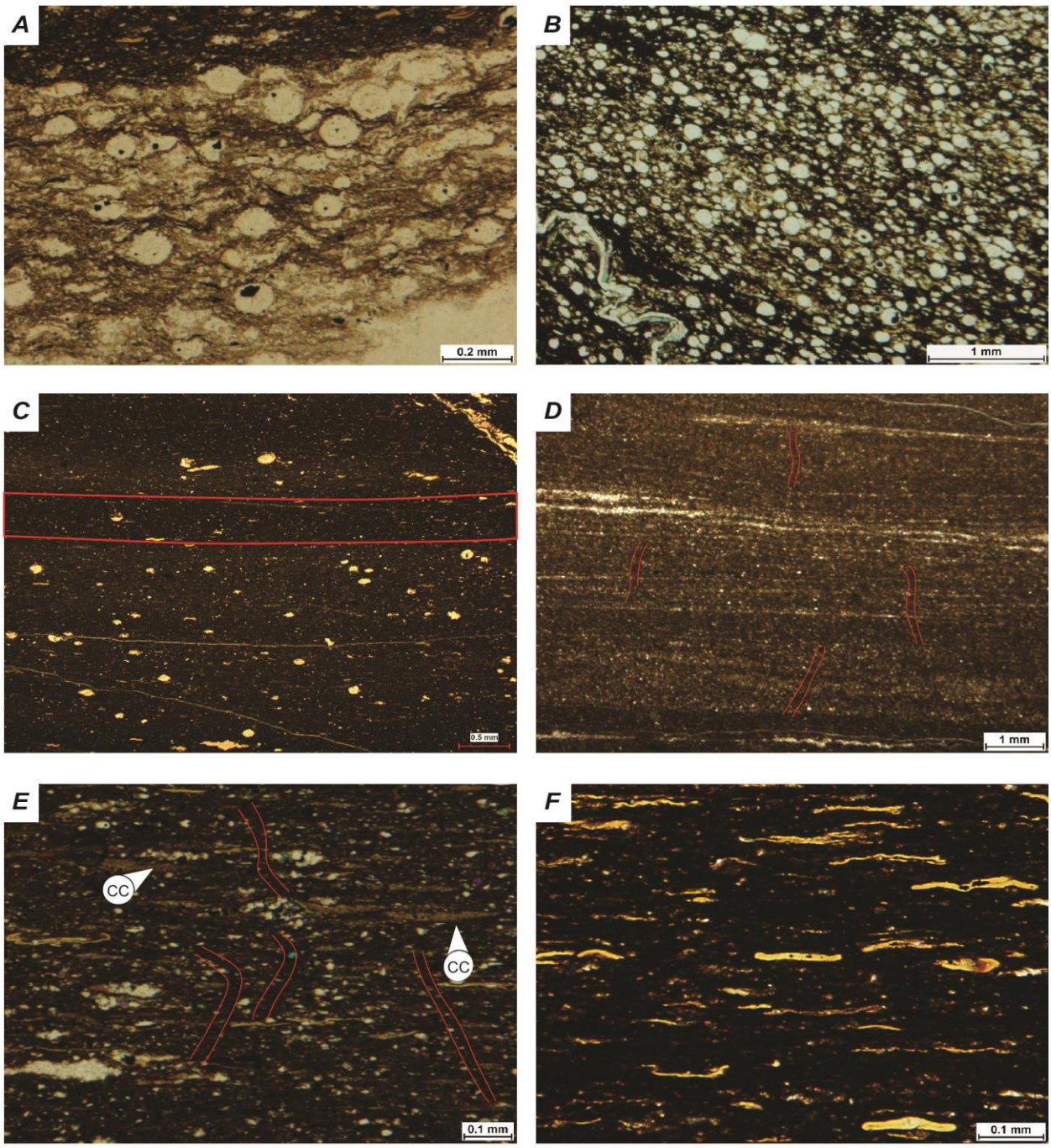

Figure 5. Facies of lower Bakken shale member: (A) Radiolarites of facies 1; EOG Resources, Inc., McAlmond 1-05H at 8853.5 ft depth; (B) Radiolaria-bearing mudstones of facies 2; Hess Corporation, IM Shorty 0805 H-1 at 7603.9 ft depth; (C) Massive, clay-rich mudstones of facies 3 highlighted in red; Hess Corporation, RS-State 3603 H-1 at 8815 ft depth; (D) Silt-bearing, massive to partially-laminated mudstones of facies 4a with *Phycosiphon incertum* fecal strings outlined in red; Brigham Oil & Gas, L.P., Olson 10-15 1H at 10667.6 ft depth; (E) Silt- and clay-clast-bearing (arrows labeled CC), partially-laminated mudstones of facies 4b with *Phycosiphon incertum* fecal strings outlined in red;

EOG Resources, Inc., McAlmond 1-05H at 8869.5 ft depth; (F) *Tasmanites*-bearing mudstones of facies 5; EOG Resources, Inc., McAlmond 1-05H at 8864.8 ft depth.

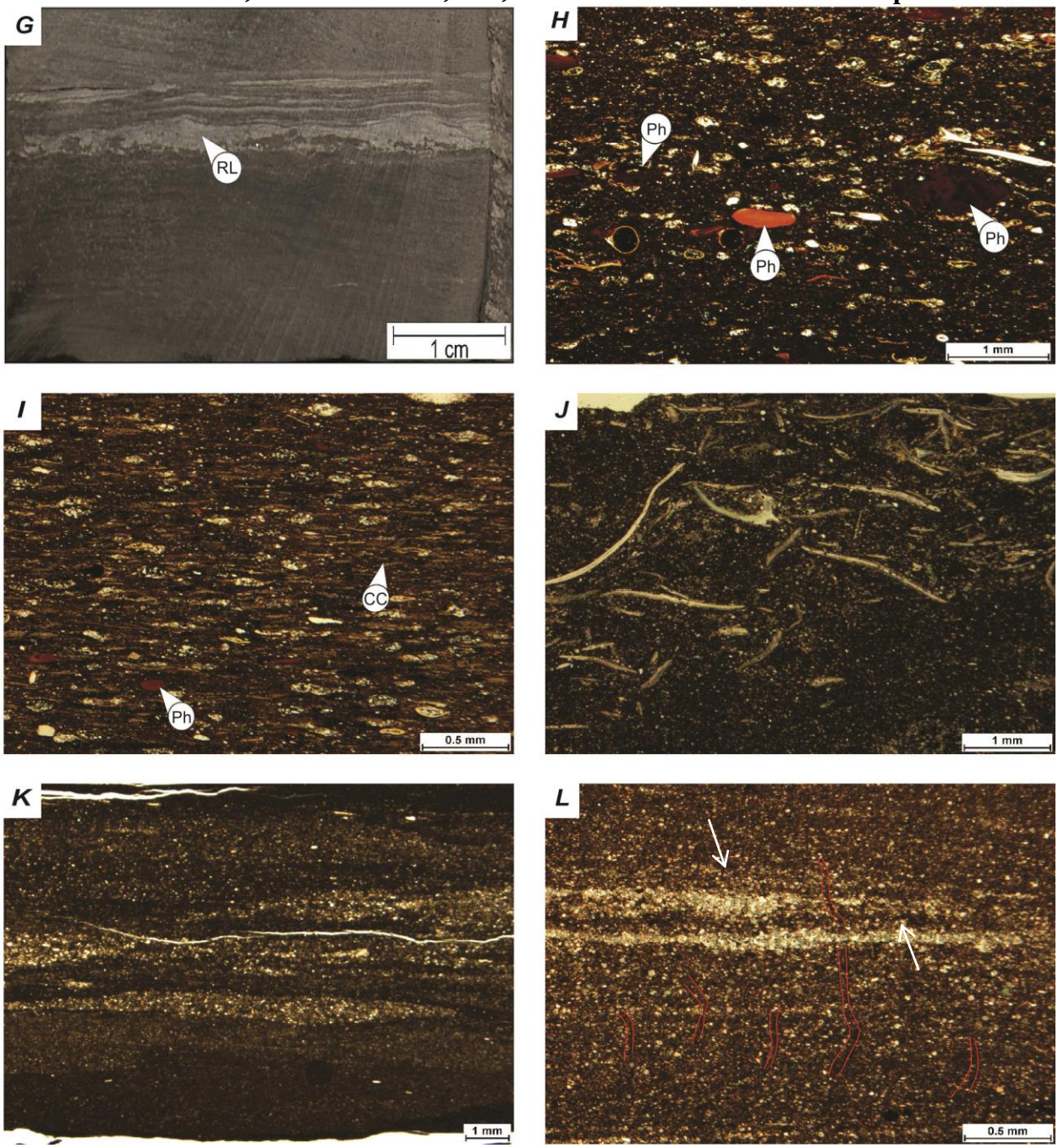

Figure 5 (Continued). Facies of lower Bakken shale member: (G) Mudstones with downlapping laminae of facies 6 (RL: ripple laminae); Amerada Hess, State of North Dakota 1-11H at 9531.4 ft depth; (H) Phosphate (Ph)- and fossil-bearing mudstones of facies 7a; Hess Corporation, RS-Nelson 1423 H-1 at 9257.5 ft depth; (I) Clay-clast (CC)-phosphate (Ph) and fossil-bearing mudstones of facies 7b; EOG Resources, Inc., McAlmond 1-05H at 8869.5 ft depth; (J) Macrofossil-bearing mudstones of facies 8; Newfield Production Company, Sergeant Major at 11114.6 ft depth; (K) Macrobioturbated

mudstones of facies 9; Newfield Production Company, Sergeant Major at 11138.2 ft depth; (L) Siltstones of facies 10 with *Phycosiphon incertum* fecal strings outlined in red; Brigham Oil & Gas, Olson 10-15 1-H at 10667.6 ft depth.

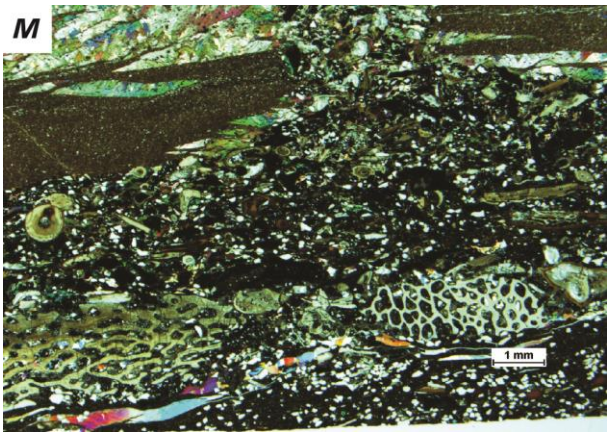

Figure 5 (Continued). Facies of lower Bakken shale member: (M) Skeletal packstones of facies 11; Newfield Production Company, Jorgenson 1-15H at 11034.6 ft depth.

4.4 Facies Associations

Table 3. Facies associations with their respective facies.

Facies Association	Facies Observed
Siliceous Black Mudstones (FA 1)	• Radiolarite (facies 1) • Radiolaria-bearing mudstone (facies 2) • Massive, clay-dominated mudstone (facies 3) • Silt-bearing, massive to partially-laminated mudstone (facies 4a) • Silt- and clay-clast-bearing, massive to partially-laminated mudstone (facies 4b)
Laminated Mudstones (FA 2)	• Radiolaria-bearing mudstone (facies 2) • Massive, clay-dominated mudstone (facies 3) • Silt-bearing, massive to partially-laminated mudstone (facies 4a) • Silt- and clay-clast-bearing, massive to partially-laminated mudstone (facies 4b) • *Tasmanites*-bearing mudstone (facies 5) • Mudstone with downlapping laminae (facies 6) • Siltstone (facies 10)
Bioturbated Mudstones with Macrofossil Debris (FA 3)	• Radiolaria-bearing mudstone (facies 2) • Silt-bearing, massive to partially-laminated mudstone (facies 4a) • Silt- and clay-clast-bearing, massive to partially-laminated mudstone (facies 4b) • *Tasmanites*-bearing mudstone (facies 5) • Mudstone with downlapping laminate (facies 6) • Phosphate- and fossil-bearing mudstone (facies 7a) • Clay-clast-, phosphate- and fossil-bearing mudstone (facies 7b) • Macrofossil-bearing mudstone (facies 8) • Macrobioturbated mudstone (facies 9) • Siltstone (facies 10)
Silt-rich Mudstones (FA 4)	• Radiolaria-bearing mudstone (facies 2) • *Tasmanites*-bearing mudstone (facies 5) • Phosphate- and fossil-bearing mudstone (facies 7a) • Clay-clast-, phosphate- and fossil-bearing mudstone (facies 7b) • Macrofossil-bearing mudstone (facies 8) • Macrobioturbated mudstone (facies 9) • Siltstone (facies 10) • Skeletal packstone (facies 11)

4.4.1 Facies Association 1 │ Siliceous Black Mudstones

FA 1 is the most common FA that also forms the thickest packages of sediment in the lower Bakken shale succession. Siliceous black mudstones are generally represented as laminae, laminasets or thin beds that can range in thickness from a few mm to approximately 30 mm and contain varying amounts of radiolarians (facies 1 and facies 2). The radiolarian deposits (facies 1 and facies 2) are commonly intercalated with laminated silt-bearing mudstones (facies 4a). Throughout this FA, laminae and thin beds of radiolaria-bearing mudstones (facies 2) commonly display planar geometries but can also exhibit variations in lateral thickness. The radiolarians are generally filled with quartz or pyrite, and rarely calcite. The matrix of laminae of the radiolarian-bearing mudstones (facies 2) contain clay minerals, detrital quartz and carbonate grains, phosphate clasts, pyrite and rare conodont fragments. Radiolarites (facies 1) are rare in FA 1 and consist primarily of compacted radiolarian remains. Pyrite concretions frequently occur isolated or in clusters throughout FA 1 and can be as large as 150 mm in length and greater than 60 mm in height, but, pyrite concretions on average are 2-20 mm in length. Continuous and discontinuous laminae of pyrite contain primarily euhedral pyrite grains with discontinuous and in some cases aligned pyrite lenses (3-15 mm in length). Additionally, thin (<1 mm), dark-brown to black laminae of massive clay-rich mudstones (facies 3) of even thicknesses are typically intercalated with light-colored, silt-bearing mudstone layers (facies 4a). Relict discontinuous laminae consisting of detrital fine- to medium-silt size grains and seldom clay clasts (facies 4a and 4b) occur rarely. These relict silt-bearing laminae are often disturbed by *Phycosiphon incertum* fecal strings that can be up to 5 mm long. This type of trace fossil also occurs in the radiolaria-bearing mudstones but is not observed in radiolarites (cf. Egenhoff and Fishman, 2013). Horizontal *Planolites* type A burrows are rare in this FA.

4.4.2 Facies Association 2 │ Laminated Mudstones

The laminated mudstones of FA 2 consists of sub-mm to 10 mm-thick laminae and beds of partially- to well-laminated silt-bearing mudstones (facies 4a and 4b) forming vertical sections that range from 0.05-3 m in thickness. The mudstone matrix consists of approximately 25-50% clay minerals, 20-45% fine- to medium-silt size siliciclastic and carbonate grains, fine-grained organic matter, 3-8% pyrite, and minor amounts of disseminated radiolarian tests, phosphate clasts, clay clasts, and conodont fragments. Phosphate clasts can be commonly found in laminae less than 4 mm in thickness with infrequent conodont fragments throughout this FA. However, in places phosphate clasts occur isolated and randomly distributed in the matrix. Siltstone (facies 10) beds and laminasets, up to 40 mm in thickness, are present but rare throughout FA 2. Locally, siltstone laminae form low-angle ripple foresets that can alternate with mud-rich laminae (facies 6). Continuous and discontinuous silt-bearing mudstone laminae (facies 4a) occur at irregular intervals in this FA and are, locally, intercalated with laminae and laminasets of radiolaria-bearing mudstones (facies 2). Radiolaria-bearing mudstones (facies 2) are mostly continuous but generally exhibit lateral variations in thickness and are discontinuous in places. They generally cluster in distinct stratigraphic intervals of 0.2-2.7 m in thickness. *Tasmanites* algae occur nearly exclusively in compacted form and occur either randomly distributed or form mm-thick, continuous grain-supported laminae (facies 5). Clay clasts commonly occur isolated but can also constitute up to 30% of mudstone laminae with quartz and carbonate silt grains and minor *Tasmanites* algae (facies 4b). *Phycosiphon incertum* fecal strings are present in all facies and often displace silt grains of silt-bearing mudstone (facies 4a) and siltstone (facies 10) laminae into the over- and underlying matrix. *Planolites* type A burrows are found predominantly in silt-bearing mudstones (facies 4a).

4.4.3 Facies Association 3 │ Bioturbated Mudstones with Macrofossil Debris

Bioturbated mudstones with macrofossil debris consist of various fossil fragments and mostly silt- and little sand-size detrital quartz and carbonate grains in a fine-grained matrix with amorphous organic matter (AOM). The macrofossil debris of this FA includes conodont fragments, crinoid stem remains, sponge pieces, and rare shell fragments. Typically, these macrofossils occur together in laminae up to 5 mm thick with sand-size phosphate clasts, detrital quartz and carbonate silt grains, *Tasmanites* algae, and clay clasts 0.08-0.5 mm in length (facies 7a and 7b). These laminae can be continuous or discontinuous and occur in places as irregular, patchy intervals throughout FA 3. Phosphate- and fossil-bearing mudstones (facies 7a and facies 7b) also exhibit rare basal scour surfaces. Partially-laminated, silt-bearing mudstone (facies 4a and facies 4b) laminae as well as continuous siltstone (facies 10) laminae can reach up to 2 mm in thickness and contain mainly sub-angular to sub-rounded detrital quartz grains. These silt-bearing mudstone and siltstone laminae are frequently intercalated with phosphate- and fossil-bearing mudstones (facies 7a and facies 7b). Locally, ripple structures (facies 6) are preserved. However, the fabric throughout FA 3 is predominantly structureless with moderate to intense bioturbation. *Planolites* type A burrows are common in the matrix, while *Planolites* type B, *Chondrites* and *Teichichnus* burrows are less frequent. *Phycosiphon* isp. and *Phycosiphon incertum* fecal strings are observed and commonly cut through phosphate- and fossil-bearing mudstones with and without clay clasts (facies 7a and 7b), while only *Phycosiphon incertum* disrupts silt-bearing mudstone laminae (facies 4a) and siltstones (facies 10).

4.4.4 Facies Association 4 │ Silt-rich Mudstones

The silt-rich mudstones of FA 4 are characterized by abundant siltstone (facies 10) laminae, laminasets and rare thin beds. Continuous and discontinuous siltstone (facies 10)

laminae and laminasets occur at irregular intervals throughout this FA. Silt-rich laminae are primarily composed of fine- to coarse-silt-size detrital quartz and carbonate grains (approximately 90-95%) and some fossil fragments in a mudstone matrix. The characteristic silt-rich (facies 10) laminae of FA 4 occur commonly intercalated with phosphate- and fossil-bearing mudstones (facies 7a and facies 7b) and/or partially-laminated silt-bearing mudstones (facies 4a and facies 4b). Laminae of 3-5% rounded and quartz-filled radiolarian tests with 10-30% silt grains in a mud matrix are rare in this FA. This is the only FA where skeletal packstones (facies 11) occur, although they are rare. In places, the siltstone (facies 10) laminae are disrupted by *Planolites* type B burrows and *Phycosiphon incertum* fecal strings. Infrequent *Teichichnus* and *Chondrites* burrows also occur in places.

4.5 Interpretation of Facies Associations

The four FAs recognized in the lower member of the Bakken Formation record deposition by both suspension and bedload processes. Throughout this unit, the occurrence of planktic radiolaria and *Tasmanites* algae cysts predominantly record deposition by settling processes under quiet-water conditions below storm wave base (Egenhoff et al., 2011; Egenhoff and Fishman, 2013). However, the presence of siltstone laminae (facies 10) with variations in lateral thickness along with clay clasts and phosphate- and fossil-bearing mudstones (facies 7a and 7b) suggest bedload transport also occurred throughout the basin, likely as storm-induced deposits (Borcovsky, 2013; Friedrichs and Wright, 2004; Macquaker et al., 2010).

Radiolarians, the principal component that make up most of the siliceous black mudstones of FA 1, were likely deposited initially through suspension settling. A quiet depositional environment would have been necessary to produce the characteristic facies, radiolarites (facies 1), of FA 1. Radiolarites (facies 1) and sub-mm laminae of clay-rich

mudstones (facies 3) exhibit even thicknesses across the width of a sample core (approximately 152 mm; 6 in), which reflects deposition by suspension processes in calm conditions. However, discontinuous and undulating radiolaria-bearing mudstone (facies 2) layers also occur in FA 1 and suggest reworking of the seafloor sediment and deposition by bed load as indicated by (1) the mixing of radiolarians with other constituents, such as mud and fine- to medium-grained silt, and (2) the laterally discontinuous laminae, which could not have been deposited by suspension processes. Similarly, rare irregular, silt-bearing mudstone laminae (facies 4a) in this FA also indicate reworking of the seafloor. The presence of clay clasts in FA 1 further implies that bedload processes were active, at least at times in FA 1, as they are interpreted to be water-rich mud particles that were eroded from the sea floor (Schieber et al., 2010).

Sediments of the laminated mudstones of FA 2 are interpreted to have been deposited in a setting of higher energy compared to that of FA 1. This interpretation is supported by a slight increase in grain size of siliciclastic and carbonate detritus, compared to FA 1, as well as a greater density of silt laminae (facies 10). Silt-bearing laminated mudstones (facies 4a) of FA 2 are frequently intercalated with sub-mm laminae of structureless clay-rich mudstones (facies 3) that are interpreted to reflect deposition by suspension settling during periods of quiescence. However, clay clasts are more abundant in FA 2 than FA 1, indicating bedload processes were more predominant in FA 2. Sedimentation of this FA by bedload processes is also supported by discontinuous and irregular siltstone laminae (facies 10) that represent distal storm-induced deposits. Also, sparse occurrences of mudstone with downlapping laminae (facies 6) composed of alternating mudstone and silt-rich laminae reflect bedload transport. In places, *Tasmanites* cysts occur with silt grains and occasional phosphate clasts in laminae that display erosional bases (facies 5), which suggests possible reworking of the sediment by bottom currents. Similar

to FA 1, though, laterally continuous laminae of *Tasmanites* cysts in FA 2 represent deposition by suspension settling processes during algae blooms (Schieber, 1996; Tappan, 1980).

The characteristic phosphate- and fossil-bearing mudstone deposits (facies 7a and 7b) of FA 3 likely represent lag deposits formed by bedload transport processes during high-energy events, such as storms. Basal scour surfaces observed in some of the phosphate- and fossil-bearing mudstone (facies 7a and facies 7b) laminae represent event-currents strong enough to erode away part of the muddy seafloor and transport this fine material further offshore. The presence of fragmented shells oriented parallel to bedding in macrofossil-bearing mudstones (facies 8) suggests transport and deposition by bedload processes. Comparable to FA 1 and FA 2, even thickness laminae of radiolaria-bearing mudstones (facies 2) occur and do reflect deposition by suspension settling processes.

Bedload transport likely caused by high-energy events, e.g. storms, is responsible for depositing most of the silt-rich mudstones of FA 4, such as siliciclastic and carbonate silt grains, together with small amounts of fine-grained sand particles. This is supported by erosive bases observed in some siltstone laminae throughout the succession, and siltstone ripple marks. The largest grain sizes of all FAs are found in FA 4 and thus have likely been deposited under the highest energy conditions of all FAs. Rare skeletal packstones observed in this FA were likely sourced from the paleoshoreline and reflect episodic sedimentation from high-energy events, such as storms that transported and deposited these coarse-grained sediments.

Abundant bioturbation from horizontally and vertically burrowing organisms disrupted much of the lower Bakken shale member sediments after deposition. The organisms that produced *Phycosiphon incertum* fecal strings displaced silt grains of silt-bearing mudstone (facies 4a and facies 4b) and siltstone (facies 10) laminae into over- and underlying sediments

(cf. Egenhoff and Fishman, 2013). The thorough reworking of mudstone deposits by these organisms throughout much of the shale succession makes it difficult to determine the original and predominant depositional process.

5.0 FACIES ARCHITECTURE

5.1 Facies Distribution

In this study, the lower Bakken shale member is subdivided into four stratigraphic units herein referred to as Intervals 1-4 (Fig. 6). These four intervals can be traced laterally through four transects (Appendices 1-4) across the entire Williston Basin in North Dakota. The four transects, two in a north-south and two in a west-east direction, display the stratigraphic and geographic distribution of all four facies associations. Interval 1 is represented by the lowermost 0-4.1 meters of the succession, but typically varies between 0.15-1.5 meters in thickness. Interval 2 overlies Interval 1 and ranges in thickness from 1.2-9.5 meters, but is commonly 3-4.5 meters thick. Interval 3 overlies Interval 2 and can be 0.3-5.5 meters thick, but generally fluctuates between 1.5-3.4 meters in thickness. Interval 4 represents the topmost 0-2 meters of the succession, and generally ranges from 0.3-0.9 meters in thickness. The contacts between the four intervals record a transition in predominant facies associations in these units, which is described in detail below.

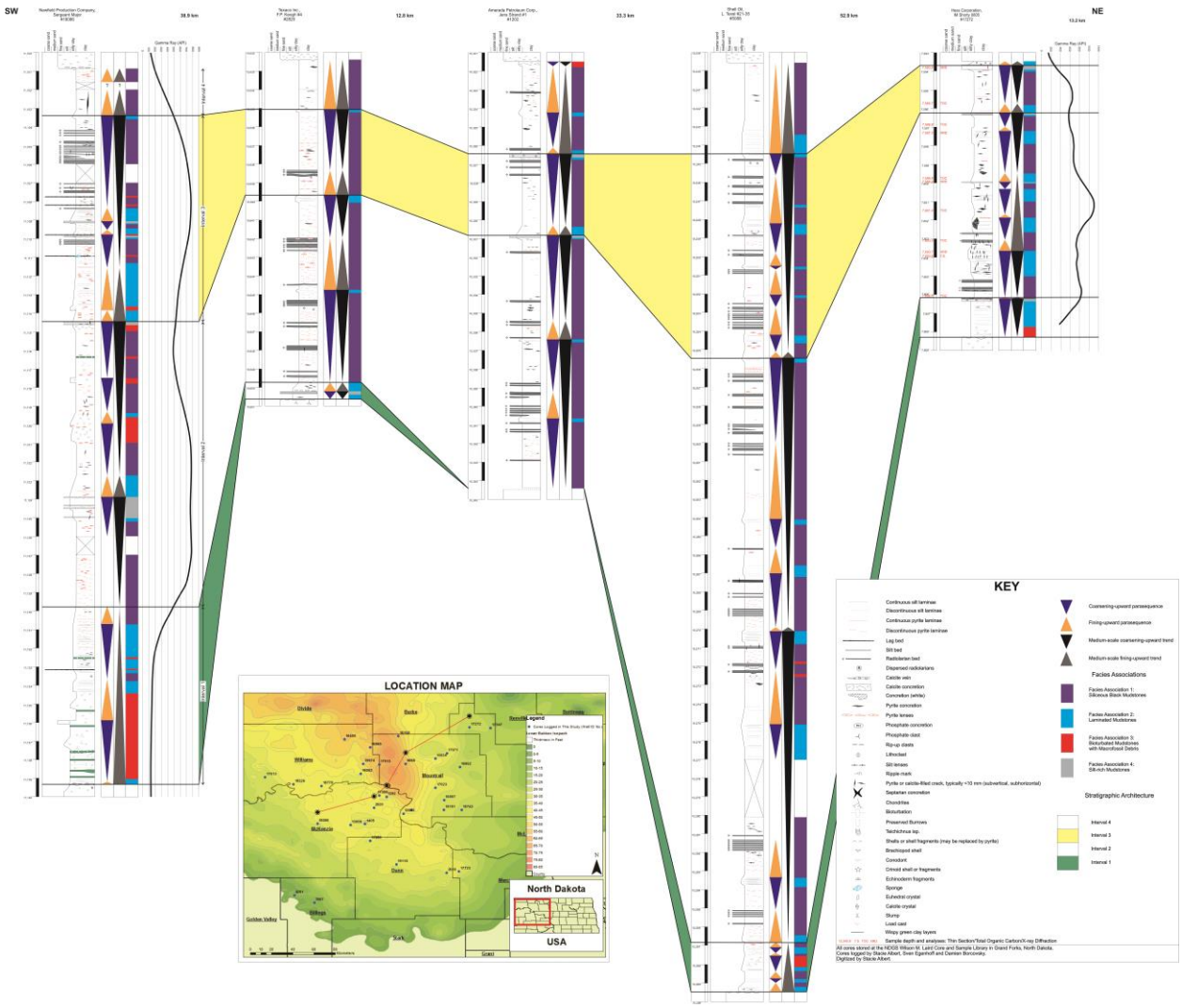

Figure 6. Transect consisting of five cores throughout the lower Bakken shale member showing detailed lithological core logs and correlation of parasequences.

5.1.1 Interval 1

Interval 1 is distinguished from the overlying Interval 2 by the predominance of FA 3 and FA 4 rocks with abundant bioturbation, fossil debris, lag deposits (facies 7a and facies 7b) and thin beds of siltstone (facies 10). This interval occurs in all cores but six that are located near the western to southwestern margin of the basin. The cores without Interval 1 display a sharp transition from the Three Forks Formation into deposits characteristic of Interval 2. Interval 1 shows one medium-scale fining-upward trend and between one and seven small-scale parasequences that can be anywhere between 0.05-2 m in thickness. The small-scale parasequences show both a fining- and coarsening-upwards in Interval 1. However, fining-upward parasequences are more dominant and typically thicker than coarsening-upward parasequences. In contrast to this general trend, though, four of the cores located near the margins of the basin show mostly coarsening-upward cycles (Appendix 4: Miller 34X-9; Appendix 3: Jorgenson 1-15H, Corrine Olson 34-20H, USA #1-24). Although the small-scale fining-upward cycles are generally thicker than the coarsening-upward cycles, their overall thickness varies between 0.075-1.6 m, and is therefore similar to the overall thickness range of the coarsening-upward parasequences. The coarsening-upward parasequences in Interval 1 always display stacking of the same facies: Fine-grained partially- to well-laminated mudstones (FA 2) at the base which generally grade upwards into siltstones (FA 4) and/or bioturbated mudstones with macrofossil debris (FA 3) at the top. Whereas, fining-upward parasequences of this interval display the reverse stacking of facies. Interval 1 also displays distinct lateral changes in facies: parasequences that contain only FA 3 and FA 4 mudstones at the basin margins grade laterally into intercalated FA 3 and FA 2 sediments and rare FA 1 mudstones toward the basin center. In general, the number of parasequences decreases towards the basin

margin. However, three cores located along the southern margin of the basin do not follow this general trend and contain an unusually thick (3-4.2 m) Interval 1 that displays an increase in the number of parasequences (e.g. Eastern North-South transect, Appendix 4, XTO Energy Inc., Miller 34X-9).

5.1.2 Interval 2

Interval 2 occurs in all cores and is commonly characterized by the intercalation of radiolaria-bearing mudstone (facies 2; FA 1) laminae with silt-bearing massive to faintly- and well-laminated mudstones (facies 4a and 4b; FA 2). In comparison with Interval 1, deposits of siltstones (facies 10; FA 4) and phosphate- and fossil-bearing mudstones (facies 7a and 7b; FA3) are less common in Interval 2, with the exception of the Marathon Oil Company, Corrine Olson 34-20H core (Appendix 3). Interval 2 displays an overall coarsening-upward trend from its base. Generally, between one and sixteen small-scale parasequences are recognized in this stratigraphic unit, and only the Marathon Oil Company's Mylo Wolding 14-11 core shows 21 small-scale parasequences (Appendix 2). In Interval 2, small-scale coarsening-upward parasequences are more common than fining-upward sediment stacks and they are generally 0.1-2.3 m thick. Small-scale fining-upward parasequences do occur, but they are rare and overall slightly thinner with thicknesses between 0.1-2 m. The increase of lower Bakken shale member thickness will lead to an increase in the thickness of individual parasequences, whereas a decrease in formation thickness will result in the opposite. All coarsening-upward parasequences generally show the same vertical facies succession with bases consisting mostly of highly-concentrated or thick (>2 mm) radiolaria-bearing mudstone layers (facies 2; FA 1) that coarsen upward into laminated mudstones (FA 2), silt-rich mudstones (FA 4) and rare intercalations of FA 3 deposits that grade near the tops. Interval 2 fining-upward parasequences

exhibit the opposite stacking of facies. The parasequences also show a distinct lateral change in facies, in which the principal deposits of Interval 2 near the basin depocenter are the siliceous black mudstones of FA 1; however, towards the margins laminated mudstones (FA 2) become thicker and more common. The number of parasequences in Interval 2 does not follow a distinct trend from proximal to distal locations in the basin and varies randomly in number from core to core.

5.1.3 Interval 3

Interval 3 displays an overall coarsening-upward trend, occurs in all cores and is bound on top and bottom by siltstone beds (facies 10), phosphate- and fossil-bearing mudstones (facies 7a and facies 7b) and/or thick (>25 mm) layers of silt-bearing laminated mudstones (facies 4a and facies 4b). Massive mudstones intercalated with abundant radiolaria-bearing mudstone laminae (facies 2) are characteristic of Interval 3 and coarsen-upward into siltstone laminae (facies 10) and thin beds near the base of Interval 4. The amount of radiolaria-bearing mudstone layers (facies 2; FA 1), in general, is greater in Interval 3 than Interval 2. However, in contrast to Interval 2, bioturbated mudstones with macrofossil debris (FA 3) are exceptionally less common in Interval 3. The distribution of siltstone laminae (facies 10) in Interval 3 does not follow a distinct trend: about half of the cores in the study area, both in the basin center as well as towards the margins, contain between 2-15% of siltstone laminae (facies 10) that are generally intercalated with radiolaria-bearing mudstones (facies 2) and massive mudstones (facies 3). One to ten small-scale fining- and coarsening-upward parasequences are recognized in Interval 3. Throughout this interval, small-scale fining-upward parasequences are as common as coarsening-upward ones and typically range from 0.1-2 m in thickness. Small-scale coarsening-upward parasequences in Interval 3 are predominantly 0.1-3.9 m thick. A characteristic

coarsening-upward parasequence in Interval 3 of the lower Bakken shale member shows abundant and/or thick (>2 mm) radiolaria-bearing mudstone layers (facies 2; FA 1) at the base, overlain by partially-laminated mudstones with or without clay clasts (FA 2), with occasional siltstones (facies 10; FA 4). Fining-upward parasequences typically display partially- to well-laminated mudstones (FA 2) at the base that grade into concentrated radiolaria-bearing mudstones intercalated with massive mudstones (FA 1). Interval 3 also shows distinct lateral facies changes from the deepest to the shallowest parts of this mudstone system. Near the basin depocenter, siliceous black mudstones (FA 1) and laminated mudstones (FA 2) are dominant. Characteristic deposits of the depocenter transition into thin (<2 mm) layers of silt-rich mudstones (FA 4), commonly intercalated with FA 1 and FA 2 deposits near the basin margins. Also, the number of parasequences decreases as Interval 3 thins towards the basin margins (Appendices 1-4).

5.1.4 Interval 4

Interval 4 overlies Interval 3 and is capped by the middle Bakken member. This interval occurs in all but two cores that are located near the southeastern margin of the basin (Appendix 4). This interval is characterized by massive mudstone (FA 1) units that can be up to 1.5 m thick intercalated with well-laminated mudstones (FA 2), bioturbated mudstones with macrofossil debris (FA 3), and/or siltstone beds (FA 4). Radiolaria-bearing mudstone deposits are less common in Interval 4 than Intervals 2 and 3. Interval 4 consists of one to three medium-scale trend(s) that display an overall fining-upward into the base of the middle Bakken member. Two to nine small-scale parasequences are recognized in this interval. The small-scale fining-upward parasequences can be 0.1-0.9 m thick and the coarsening-upward parasequences 0.1-1.5 m in thickness. Massive mudstones (FA 1) comprise the base of coarsening-upward parasequences

that grade into silt-rich mudstones (FA 4) and phosphate- and fossil-bearing mudstone (facies 7a and 7b) deposits of FA 3 at the top. Fining-upward parasequences display the opposite vertical stacking of facies. Laterally, FA 1 and FA 2 deposits are commonly intercalated near the basin's depocenter with occasional FA 3 and FA 4 deposits, while near the basin margins, bioturbated and fossil-bearing mudstones (FA 3) and silt-rich mudstones (FA 4) are more frequent and can occur as thick (>2 mm) deposits. In general, the number of parasequences decreases towards the basin margins; however, two cores on the western margin of the basin show an increase in parasequences (Appendix 1).

5.2 Distribution of Silt-rich and Radiolaria Facies

Stratigraphically, silt laminae (facies 10) are most abundant in Interval 1 and decrease in abundance through Interval 3. Silt content increases slightly in Interval 4 before the contact with the middle Bakken member (Table 4, Fig. 7A-D). Laterally, high silt content is pronounced in the north-northeast and southern regions of the study area. Low silt percentages are found in the northwest part of the study area, with the exception of Interval 1 where silt is abundant throughout the region.

Table 4. Average percent of silt content for each entire interval.

Interval	Average Percent of Silt For Entire Interval (Average of All Cores)
1	26.5%
2	10.2%
3	6.8%
4	8.7%

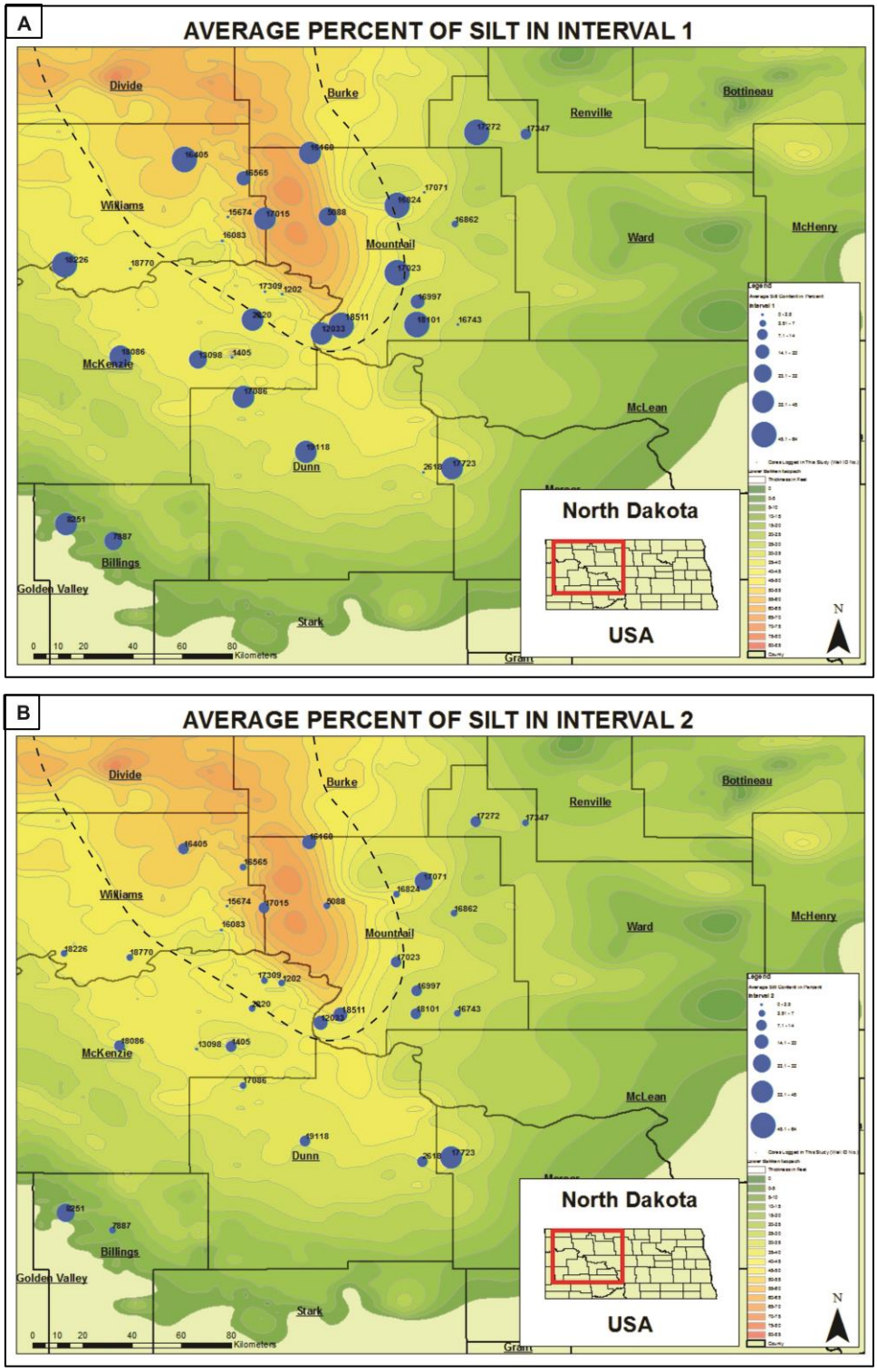

Figure 7. Isopach map of the lower Bakken shale member showing the percentage of rock that consists of siltstone (facies 10) laminae in the laminated mudstones of FA 2 and silt-rich mudstones of FA 4. Cores are identified by well ID number. Generalized lower

Bakken shale member depocenter is represented by the dashed line. (A) Average percent of silt per well in Interval 1; (B) Average percent of silt per well in Interval 2.

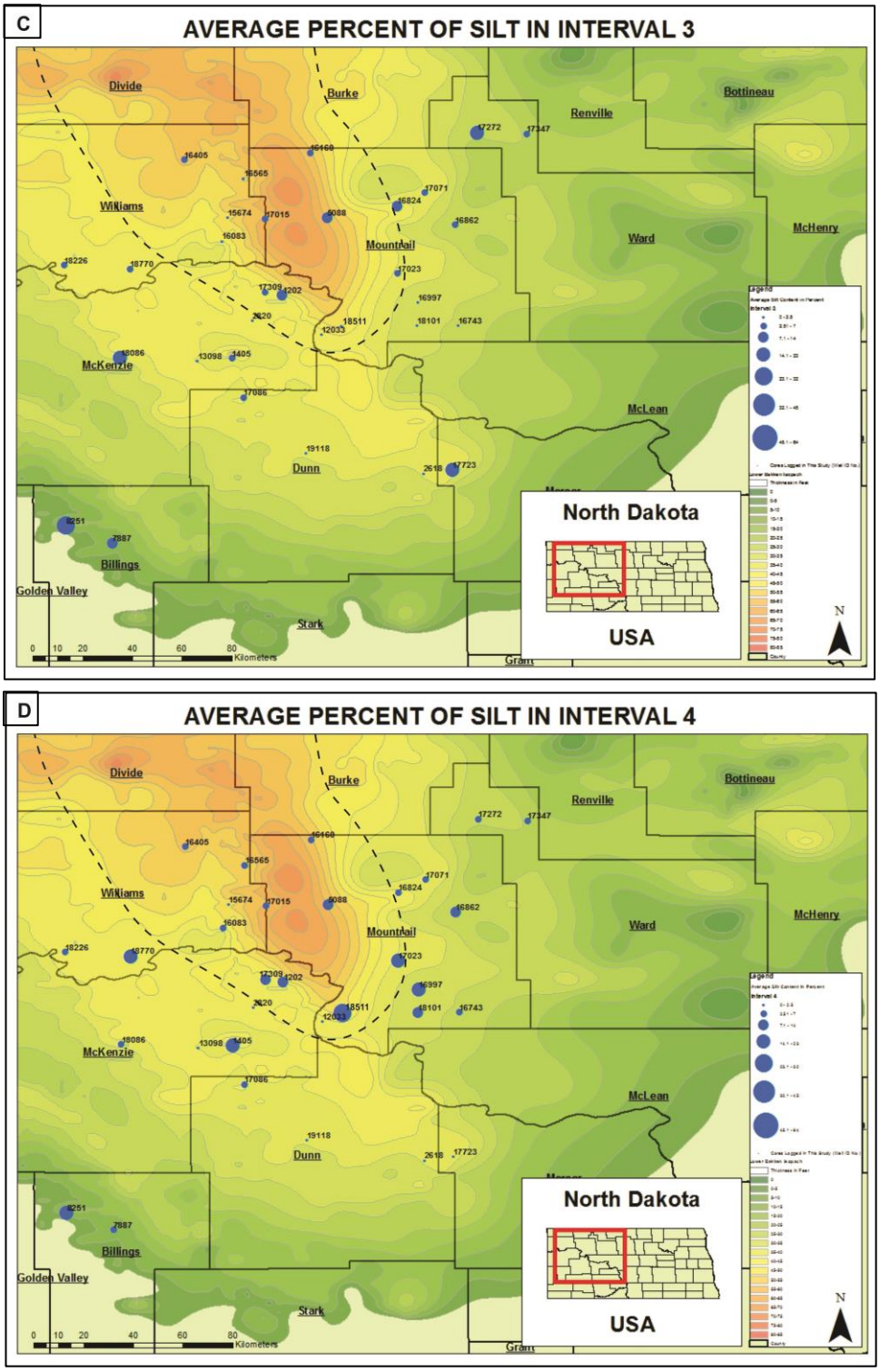

Figure 7 (Continued). (C) Average percent of silt per well in Interval 3; (D) Average percent of silt per well in Interval 4.

In most cores, intercalated laminae of radiolarites (facies 1) and radiolaria-bearing mudstones (facies 2) are greatly more abundant in Intervals 2 and 3 (Table 5). Geographically, radiolarians are more prevalent in the depocenter as well as closely surrounding the south-southeastern edge of the depocenter. Low abundances of radiolarites (facies 1) and radiolaria-bearing mudstones (facies 2) generally occur near the basin margins. In Figure 8A-D, the average number of radiolarite (facies 1) and radiolaria-bearing mudstone (facies 2) laminae per foot in each respective interval are shown.

Table 5. Average number of radiolarite (facies 1) and radiolaria-bearing mudstone (facies 2) laminae per foot for each entire interval.

Interval	Average Number of Facies 1 and Facies 2 laminae/ft for Entire Interval (Average of All Cores)
1	0.09 laminae/ft
2	1.33 laminae/ft
3	1.49 laminae/ft
4	0.60 laminae/ft

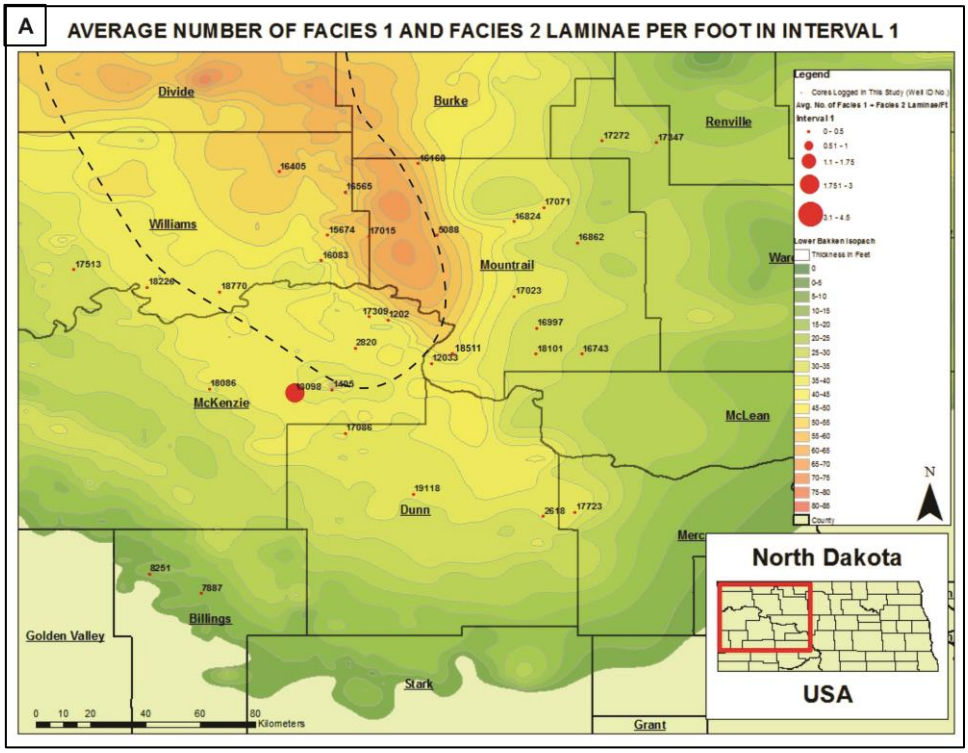

Figure 8 (Previous Page). Isopach map of the lower Bakken shale member showing the average number of radiolarite (facies 1) and radiolaria-bearing mudstone (facies 2) laminae per foot in each stratigraphic interval. Cores are identified by well ID number. Generalized lower Bakken shale member depocenter is represented by the dashed line. (A) Average number of facies 1 and facies 2 laminae per foot in Interval 1.

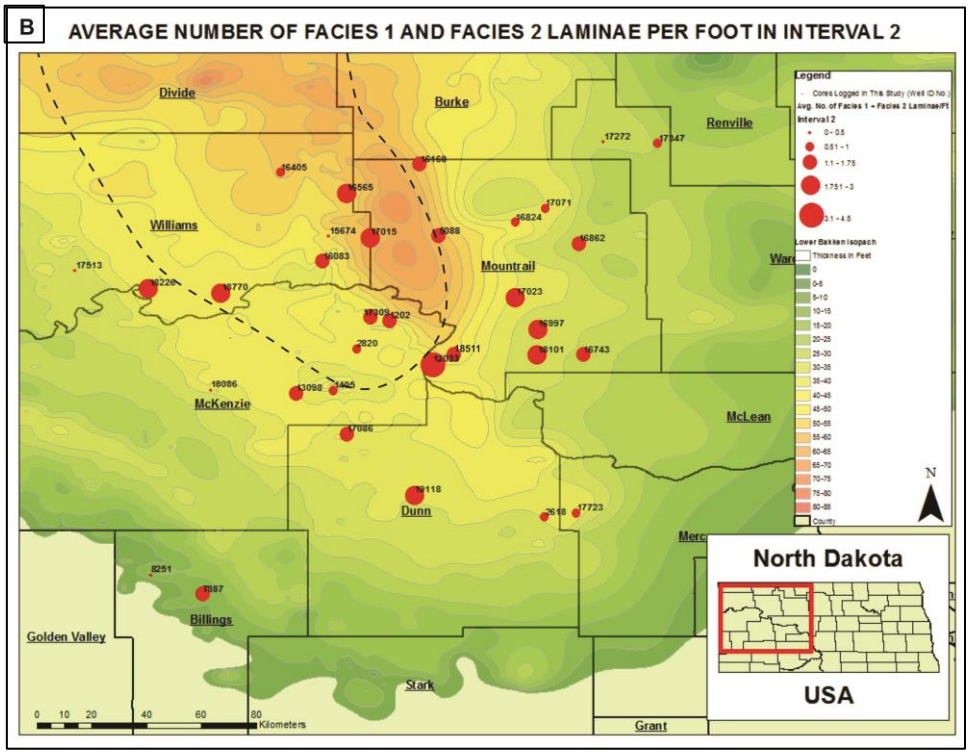

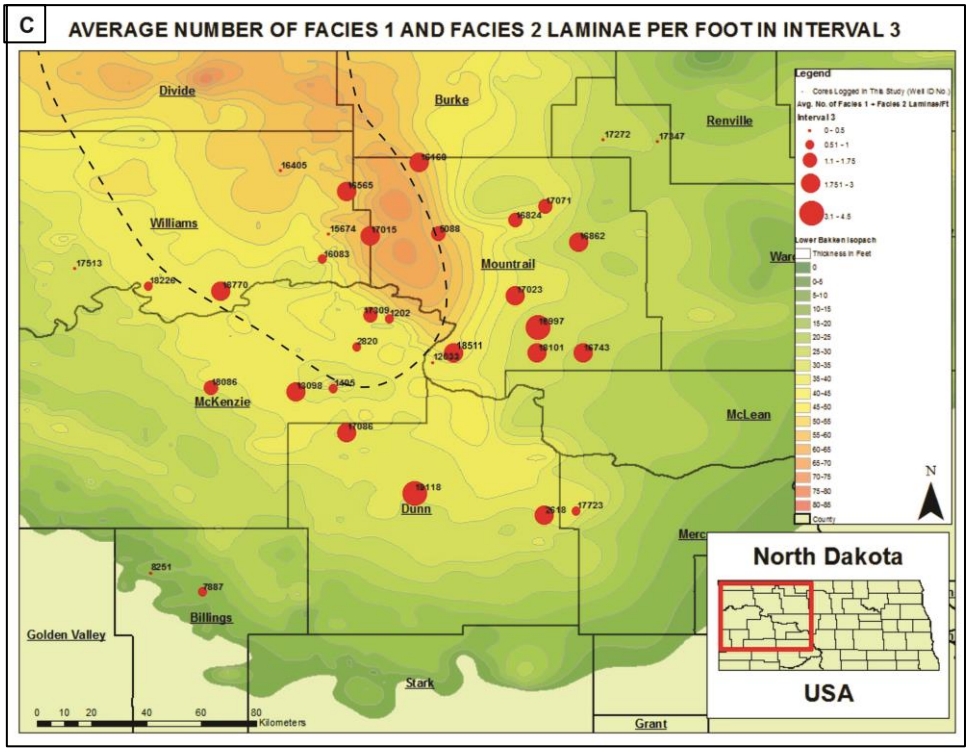

Figure 8 (Continued; Previous Page). (B) Average number of facies 1 and facies 2 laminae per foot in Interval 2; (C) Average number of facies 1 and facies 2 laminae per foot in Interval 3.

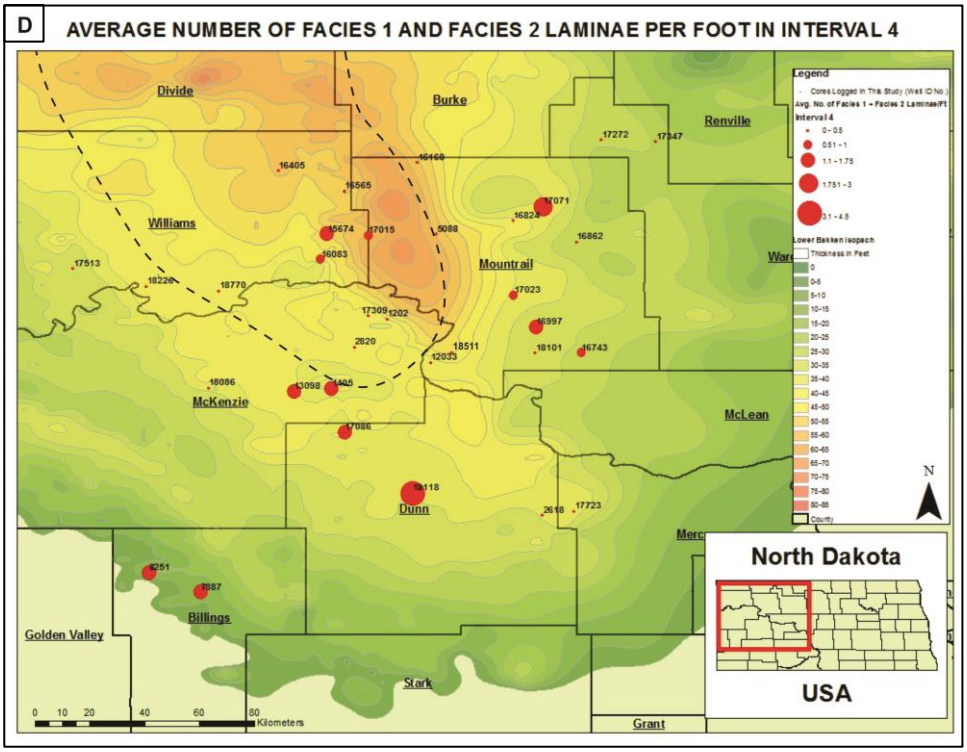

Figure 8 (Continued). (D) Average number of facies 1 and facies 2 laminae per foot in Interval 4.

6.0 GAMMA RAY (GR) LOGS AND TOTAL ORGANIC CARBON (TOC)

Total gamma ray (GR) logs for twenty-four of the cores logged in this study were used to assist in stratigraphic correlations and to examine how the amount of radioactive isotopes change throughout the lower Bakken shale succession (Appendices 1-4). These GR logs were obtained as downloadable LAS files from the North Dakota Geological Survey website. The depths on the GR logs commonly do not match the depths on the drill core and have been shifted accordingly to match the upper and lower contacts of the lower Bakken shale member.

The GR curve generally shows 5-6 maxima and 4-5 minima in most cores throughout the entire thickness of the shale succession. The highest GR values of the lower Bakken shale member occur at the base of the succession near the transition from the underlying Three Forks Formation into the lower shale, where GR values range between 800 and 1000 API units. Similarly, Interval 3 records a strong gamma ray response with values reaching approximately 750-850 API units in massive mudstones (facies 3 and facies 4a) intercalated with radiolaria-bearing mudstones (facies 2). The lowest gamma ray response of the entire shale succession with GR values between 150 and 400 API units typically occurs in places throughout Interval 1, where this unit is thick and dominated by heavily bioturbated mudstones with macrofossil debris (FA 3). These local low GR values of Interval 1 occur just above the initial high GR response that marks the base of the lower Bakken shale member. Low GR values of 250-400 API units also occur in a 0.5-2 m thick section near the middle portion of Interval 2 in massive and siliceous mudstones (FA 1). As an exception, however, is the Hess Corporation, IM Shorty 0805H-1 core near the basin margin. The highest GR values (1100 API units) of the entire core are found in the middle portion of Interval 2. Overall, separate from the areas of highest and

lowest GR response, the GR log generally ranges between 400 and 700 API units for the lower Bakken shale member.

Forty-two samples from four cores (well ID #'s: 16160, 17015, 17023, 17272) were analyzed for TOC and values for these samples range from 1.16 to 20.4% (Fig. 9; Appendix 6 for TOC data). Rock-Eval pyrolysis completed on one sample from each core (total of four) indicates that these wells are located within the oil window (Fig. 10). Three of the wells tested (16160, 17015, 17272) are thermally mature, but the Whiting Oil and Gas Corporation Braaflat 11-11H well (17023) is "immature," as indicated by its hydrogen index (HI) value (Sonnenberg, 2011). The HI of a source rock reflects oil-generative potential and is inversely proportional to the source rock's thermal maturity (McCarthy et al., 2011).

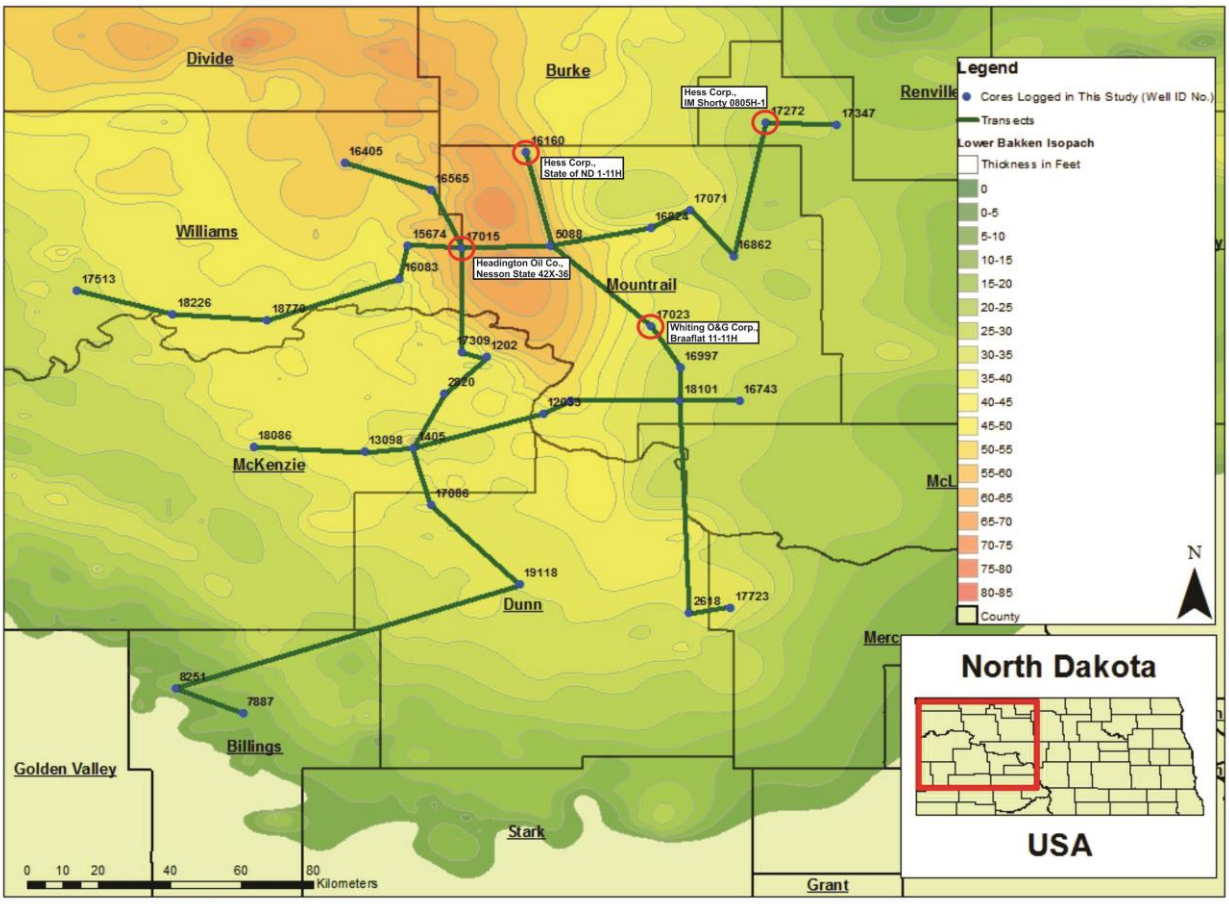

Figure 9. Isopach map of the lower Bakken shale member showing the location of the two cores samples for TOC analysis. The cores are labeled with their well ID numbers.

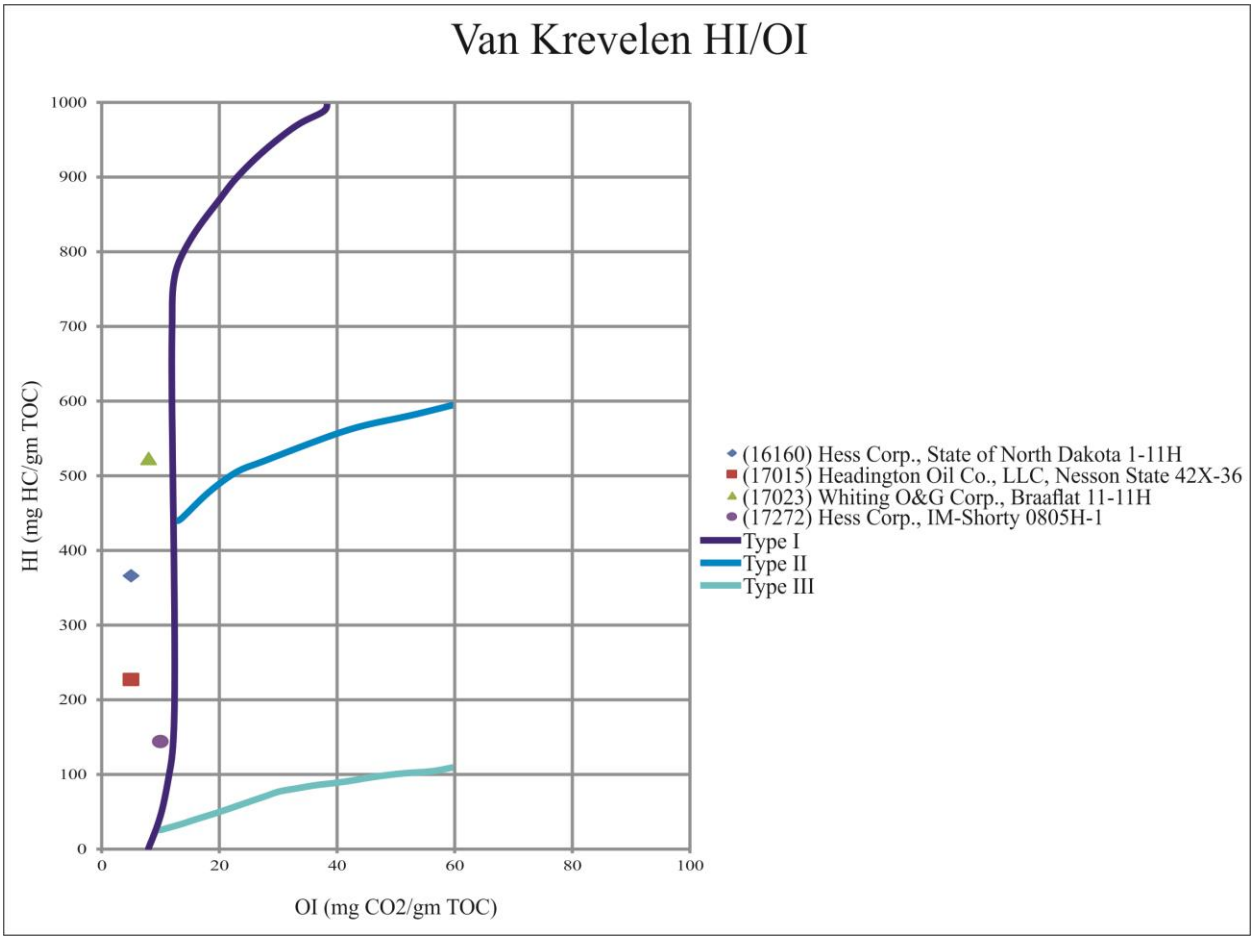

Figure 10. Modified Van Krevelen diagram from Sonnenberg (2011) for the lower Bakken shale member. The samples indicate a Type-I oil-prone kerogen (algal origin). Legend shows sample well ID number, operator and name.

Thirty-eight of the forty-two TOC samples consist mainly of massive to partially-laminated mudstones and few radiolarian-bearing mudstones (FA 1) selected primarily from the base of coarsening-upward parasequences over the entire thickness of the lower Bakken shale succession. Three of the cores sampled (#16160, Fig. 11; #17015, Fig. 12; #17023, Fig. 13) are located near the basin depocenter and display an overall trend of increasing TOC from the base to the top of the succession. However, Hess Corporation's IM-Shorty 0805H-1 (#17272; Fig. 14) core located near the basin margin exhibits the reverse trend, with decreasing TOC values from the base to the top of the succession. The overall highest TOC data are found in the

massive mudstones of FA 1 in samples across Interval 4, which have values between 14.7 and 18.5%. Samples across Intervals 2 and 3 show slightly lesser amounts of organic matter with TOC contents between 3 and 20.4%, whereas samples of massive to partially-laminated mudstones (FA 1) of Interval 1 have the lowest overall TOC values between 1.2 and 6.7%. The remaining four TOC samples analyzed consist of well-laminated mudstones of FA 2, two from Interval 3 and two from Interval 2, and have TOC values between 5.3% and 13.7%.

Figure 11 (Next Page). Litholog of Hess Corp., State of ND 1-11H (well #16160) core with gamma ray log and TOC data. As with well #'s 17015 and 17023, #16160 shows an overall increase in TOC content upsection.

Figure 12 (Page 44). Litholog of Headington Oil Company, Nesson State 42X-36 (well #17015) core with gamma ray log and TOC data. Note the overall increase in TOC content towards the top of the succession.

Hess Corporation, State of North Dakota 1-11H
#16160

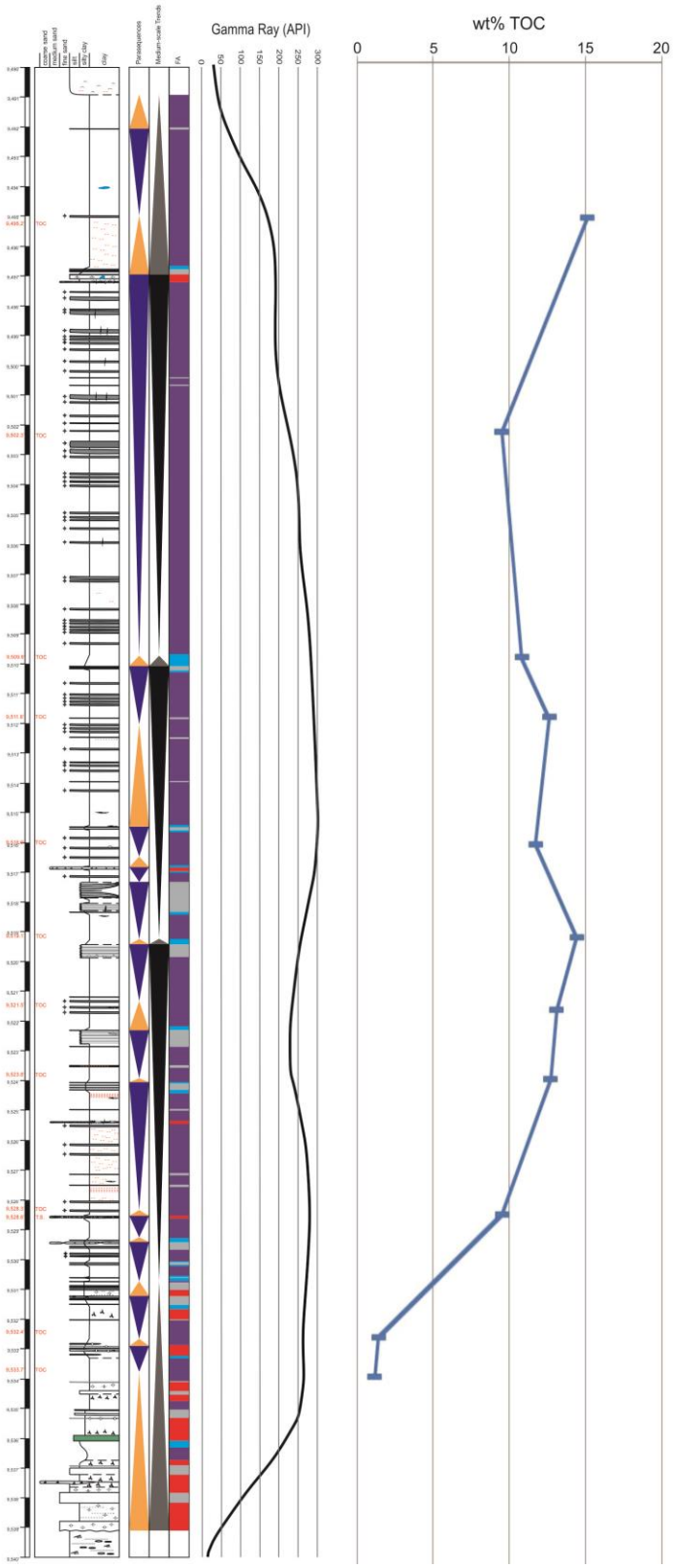

Headington Oil Co., Nesson State 42X-36
#17015

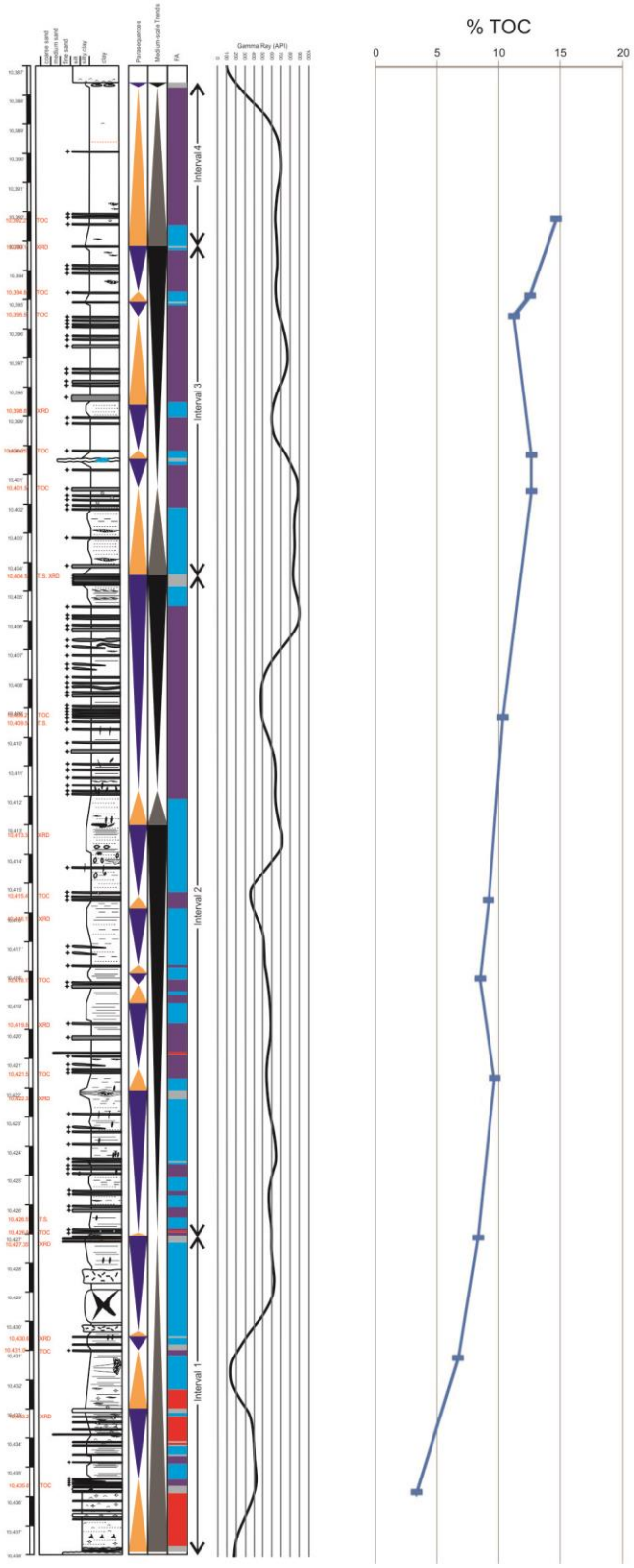

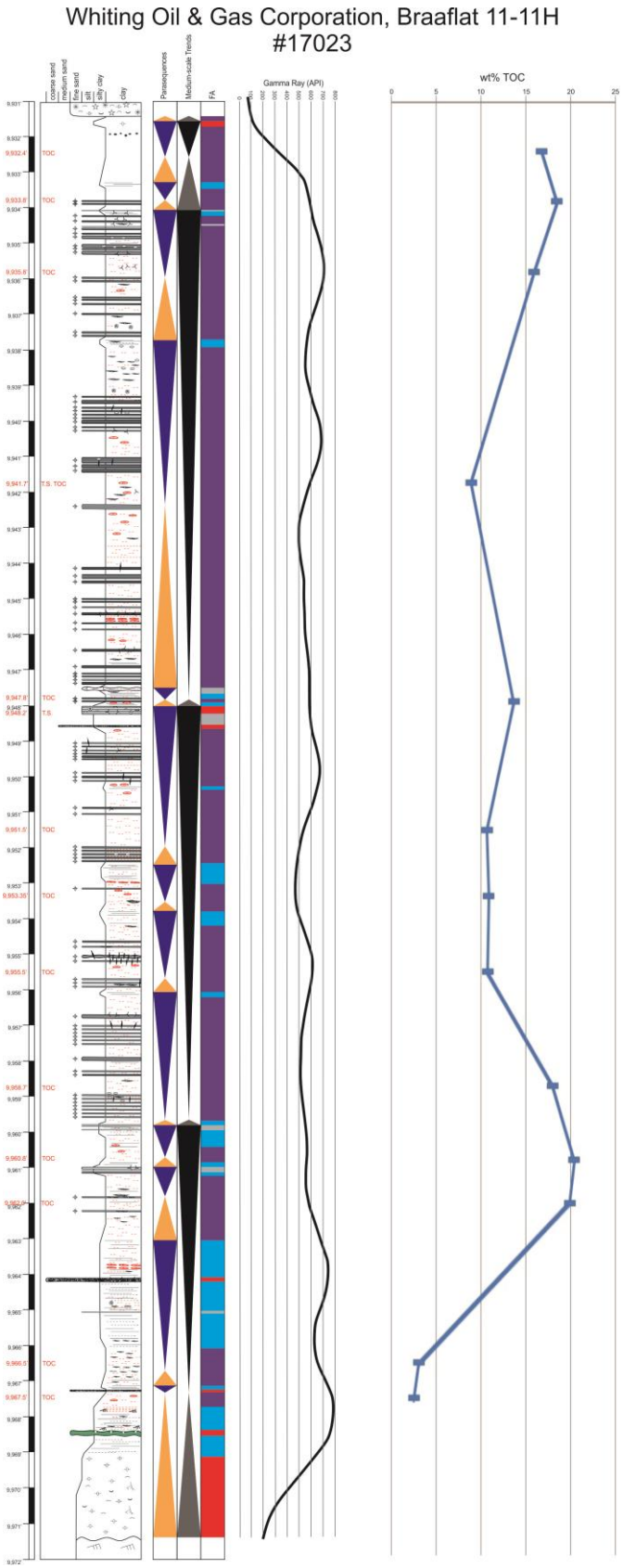
Whiting Oil & Gas Corporation, Braaflat 11-11H
#17023
coarse sand
medium sand
fine sand
silt
silty clay
clay
Parasequences
Medium-scale Trends
FA
Gamma Ray (API)
wt% TOC
0
5
10
15
20
25
TOC
T.S. TOC
T.S.

Figure 13 (Previous Page). Litholog of Whiting Oil & Gas Corp., Braaflat 11-11H (well #17023) core with gamma ray log and TOC data. Note the overall increase in TOC content towards the top of the succession.

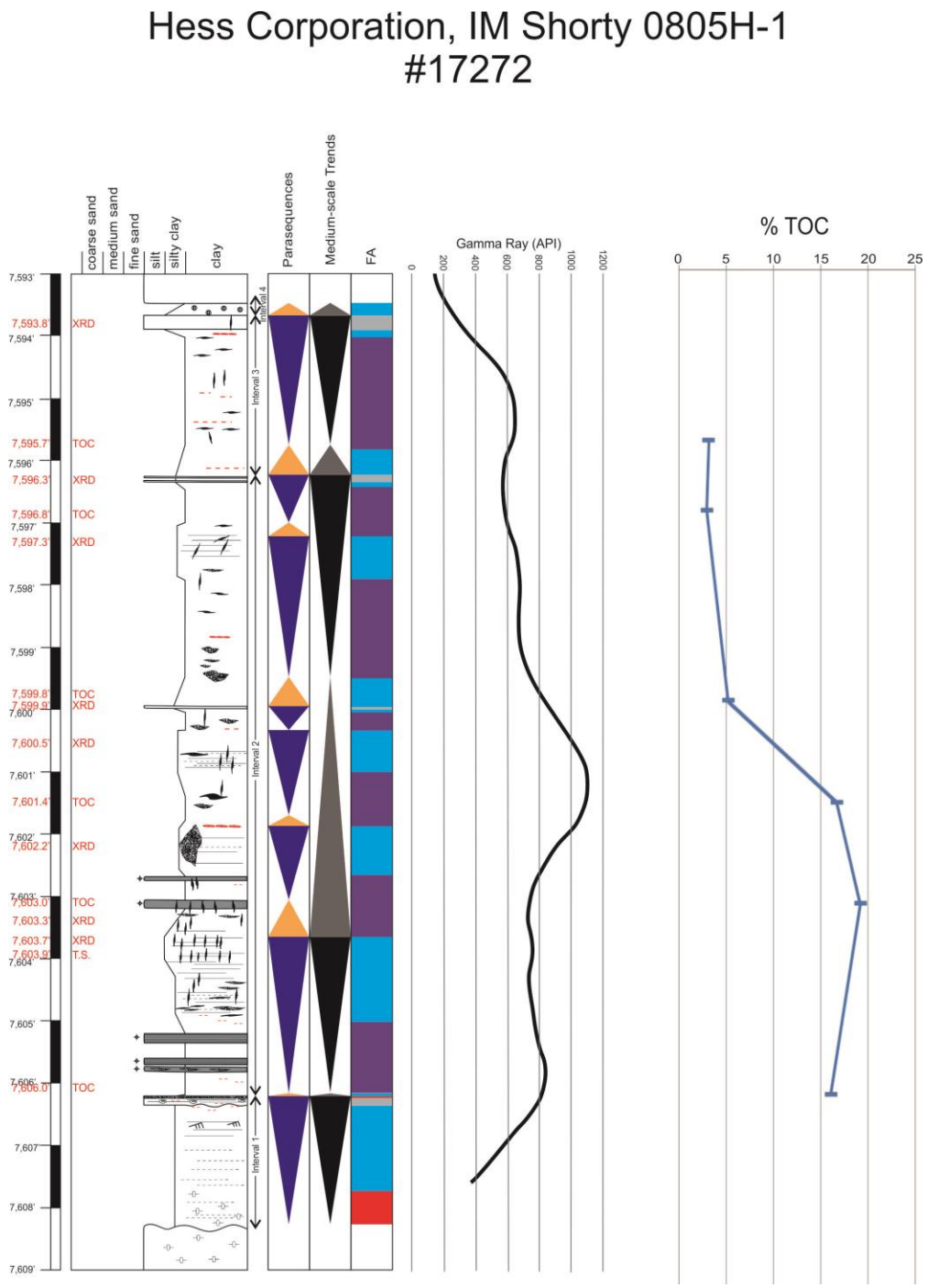

Figure 14. Litholog of Hess Corporation, IM Shorty 0805H-1 (well #17272) core with gamma ray log and TOC data. Note the overall decrease in TOC content towards the top of the succession.

7.0 INTERPRETATION

7.1 Depositional Model

The Upper Devonian lower Bakken shale member is here interpreted as representing the mud-rich distal end of a mixed carbonate siliciclastic ramp (Borcovsky, 2013; Egenhoff et al., 2011; Egenhoff and Fishman, 2013). The four FAs recognized in this succession reflect decreasing energy conditions from proximal to distal along this ramp transect (Fig. 15A-B).

The most proximal of the four lower Bakken shale member FAs are the silt-rich mudstones of FA 4 predominately located in the southern and north to northeastern portions of the basin. They are characterized by abundant indicators for high-energy conditions in mudstones, such as large phosphate clasts, fossil debris and clay clasts, as well as erosional bases with and without mm-deep scours (cf. Egenhoff and Fishman, 2013; Schieber et al., 2010). In places, carbonate shells accumulated together with carbonate mud forming patches of skeletal packstone (facies 11). Locally, high-energy sediments of FA 4 are intercalated with mud-rich laminae and beds, the coarse-grained deposits probably representing sedimentation during storm events, whereas the intercalated bioturbated mudstones reflect quiet-water deposition during fair weather conditions. The siliciclastic and carbonate detritus for this most proximal FA is most likely derived from proximal portions of this sedimentary system, as suggested by Egenhoff and Fishman (2013) for the upper Bakken shale member. Relatively high energy often corresponds with slightly better oxygenated conditions, which is reflected in thorough bioturbation of the sediments and is best seen in the bioturbated siltstones (facies 10) (cf. Egenhoff and Fishman, 2013; Tyson and Pearson, 1991).

FA 3 mudstones are overall finer-grained and darker-colored than the most proximal FA 4 lower Bakken shale deposits. The finer overall grain sizes of FA 3 reflect an overall decrease in depositional energy. FA 3 sediments are comprised of high energy sediments like FA 4, such as phosphate clasts, conodonts, clay clasts and fine- to coarse-silt size detrital siliciclastic and carbonate grains occurring as laminae (facies 10), but also contain sediments typical in low energy settings, such as massive mudstones that may display relict laminae (facies 4a). In FA 3, fine-grained material intercalated with coarse-grained sediments reflects deposition in an overall low energy setting affected by periodic high energy events. Clay clasts observed in this FA formed by erosion of up-dip clay-rich sediment and were deposited by bottom currents, likely during infrequent storms (Schieber et al., 2010). Also, the presence of ripple structures (facies 6) is consistent with deposition by storm-induced currents that transported primarily silt grains and mud floccules. Such storm-influenced currents are most likely also responsible for the deposition of siltstone laminae (facies 10) with variations in lateral thickness. Stronger storms were more infrequent and produced tempestite beds consisting of macrofossils, conodonts and phosphate clasts.

Laminated mudstones of FA 2 represent deposits basinward of FA 3 and are characterized by mostly tranquil sedimentary conditions interrupted by high energy events, e.g. episodic storms, which deposited sediments such as clay clasts, phosphate clasts and conodonts. However, unlike FA 3, the overall occurrence of coarse-grained material is less common in FA 2, which is a result of currents that already deposited much of the coarse sediment load in the more proximal reaches of the depositional transect. Additionally, the rare presence of ripple structures (facies 6) is consistent with the infrequent occurrence of high energy events in a generally low energy setting.

FA 1 deposits have the finest grain size of all lower Bakken shale member sediments and therefore are interpreted to represent the most distal portion of the depositional transect. Even though this environment represents the basin center during lower Bakken shale deposition, both suspension and bedload processes characterized this environment. Suspension deposition of clay particles or floccules most likely produced the sub-mm thick, clay-rich mudstone laminae (facies 3) found in this FA, whereas, currents that could travel to these distal settings generally carried fine silt grains. Strong storms likely transported and deposited rare coarser-grained sediments to this part of the basin, such as medium- to coarse-grained silt particles. Consequently, distinct storm-produced silt laminae are rare in the massive to partially laminated mudstones (facies 4a and 4b) present in FA 1. Radiolarites (facies 1) could only accumulate in the distal reaches of the basin where quiet water conditions allowed them to accumulate from suspension settling. Currents that reached these distal regions reworked some of these radiolarite (facies 1) deposits and mixed the radiolarian microfossils with sediment available in the flow, generally mud and very fine- to fine-grained silt (facies 2) (Egenhoff and Fishman, 2013). However, as the bulk of FA 1 deposits are highly disrupted by *Phycosiphon incertum* fecal strings resulting in mostly massive and not well-defined laminae, the predominant depositional process for much of FA 1 remains unclear.

Tasmanites algae occur in high concentrations across most of the marginal lower Bakken shale member facies (Table 2). These algal cysts originate from algae blooms in the water column, much like radiolarian blooms (Tappan, 1980). However, they seem to be linked with shallower waters than the radiolarians, as abundant accumulations of the algae occur mainly near the basin margins. The *Tasmanites* algae generally do not occur with the radiolarians, likely because they provide a potential food source for the latter (cf. Bohacs et al., 2005). As a result of

the highly resistant nature of their cyst walls to chemical breakdown (Schieber, 1996), *Tasmanites* algae are well preserved throughout the shale succession. *Tasmanites* algae occur in two preservation styles throughout the lower Bakken shale member succession: infilled and flattened. Preserved infilled *Tasmanites* cysts are less common than their collapsed counterparts, but are likely indicative of slow sedimentation rates because those conditions allow for the best chance of the deposited cysts to fill with diagenetic minerals before compactional collapse (Schieber, 1996). Continuous laminae of infilled *Tasmanites* therefore most likely suggest periods of low sediment accumulation, which favored the filling of the algal cysts during early diagenesis (Schieber, 1998b). Infilled *Tasmanites* are commonly present near transgressive surfaces in the lower Bakken shale succession, when much of the sediment load was deposited in the most proximal settings, leaving the offshore areas sediment-starved (Coe et al., 2003). It is likely, then, that compaction caused flattening of the *Tasmanites* walls when sedimentation rates increased.

Abundant bioturbation in all lower Bakken shale member FAs implies that the entire basin was largely habitable. However, the diversity of trace fossils decreases from the most proximal deposits of FA 4 towards the deepest portions of the basin (FA 1). *Chondrites*, *Teichichnus* and *Planolites* type A and B burrows are present in the proximal strata of FA 4, along with *Phycosiphon* fecal strings, whereas, in the distal FA 1, only minor *Planolites* type A burrows and moderate *Phycosiphon incertum* occur. This decrease in trace fossil diversity likely reflects diminishing oxygen content downramp (cf. Egenhoff and Fishman, 2013), where bottom water conditions in FA 4 were occasionally oxic and in FA 1, conditions were dysoxic to rarely anoxic, as indicated by the occurrence of radiolarites (facies 1) that lack any evidence of bioturbation (cf. Egenhoff and Fishman, 2013).

Along the depositional transect, the preservation of sedimentary structures is likely a function of the relationship between bioturbation extent and sediment accumulation rate. The presence of bioturbation across all FAs indicates that sedimentation rates at times were low enough to allow organisms to burrow in the sediment (cf. Borcovsky, 2013; Egenhoff and Fishman, 2013). *Phycosiphon incertum* fecal strings destroyed much of the laminated fabric found in the distal reaches of FA 1 and FA 2. This suggests that sedimentation rates in the distal offshore areas of the basin were lower than in FA 3 and FA 4, where higher sedimentation rates allowed sedimentary structures to be better preserved before disruption by burrowing organisms.

Areas of high sediment accumulation throughout the lower Bakken shale correspond to localities that have an overall high silt content (facies 10). The increase in the silt content of the rocks most likely reflects the distal expression of the sediment input locations into this basin, one in the north to northeast, along with one possible source of detritus in the southern portion of the study area (Marathon Oil Co., Mylo Wolding 14-11; Appendix 2). It is therefore most likely that two deltas were located in the northeastern and southern portions of the basin during lower Bakken shale times. The detrital sediment was likely sourced from the Acadian Mountains to the east and cratonic highlands to the north and northeast that are thought to be highlands in the Late Devonian and Early Mississippian (Smith and Bustin, 1998).

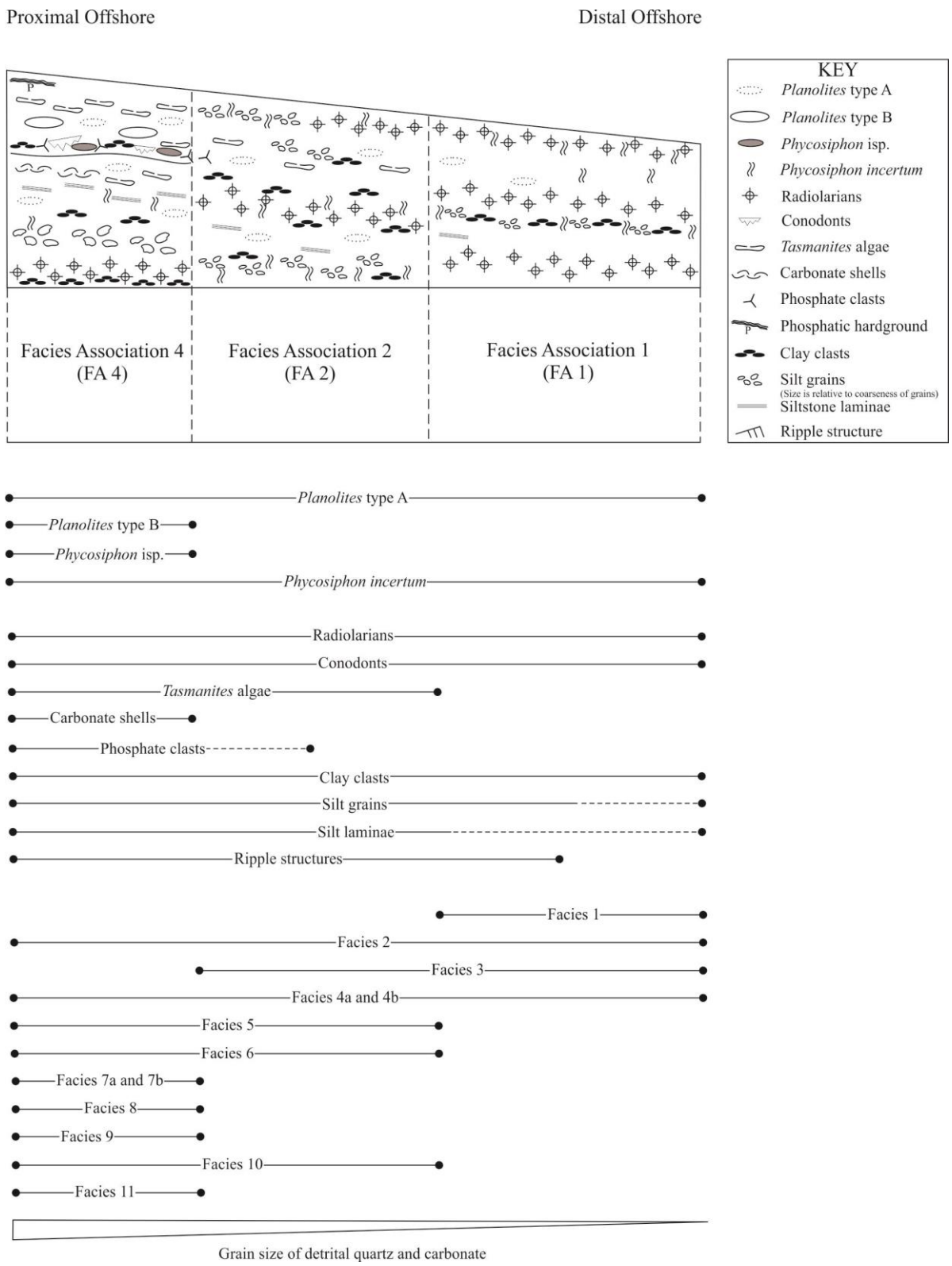

Figure 15A. Depositional model for the lower Bakken shale member in the southern and northeastern portions of the study area (Modified from Egenhoff and Fishman, 2013).

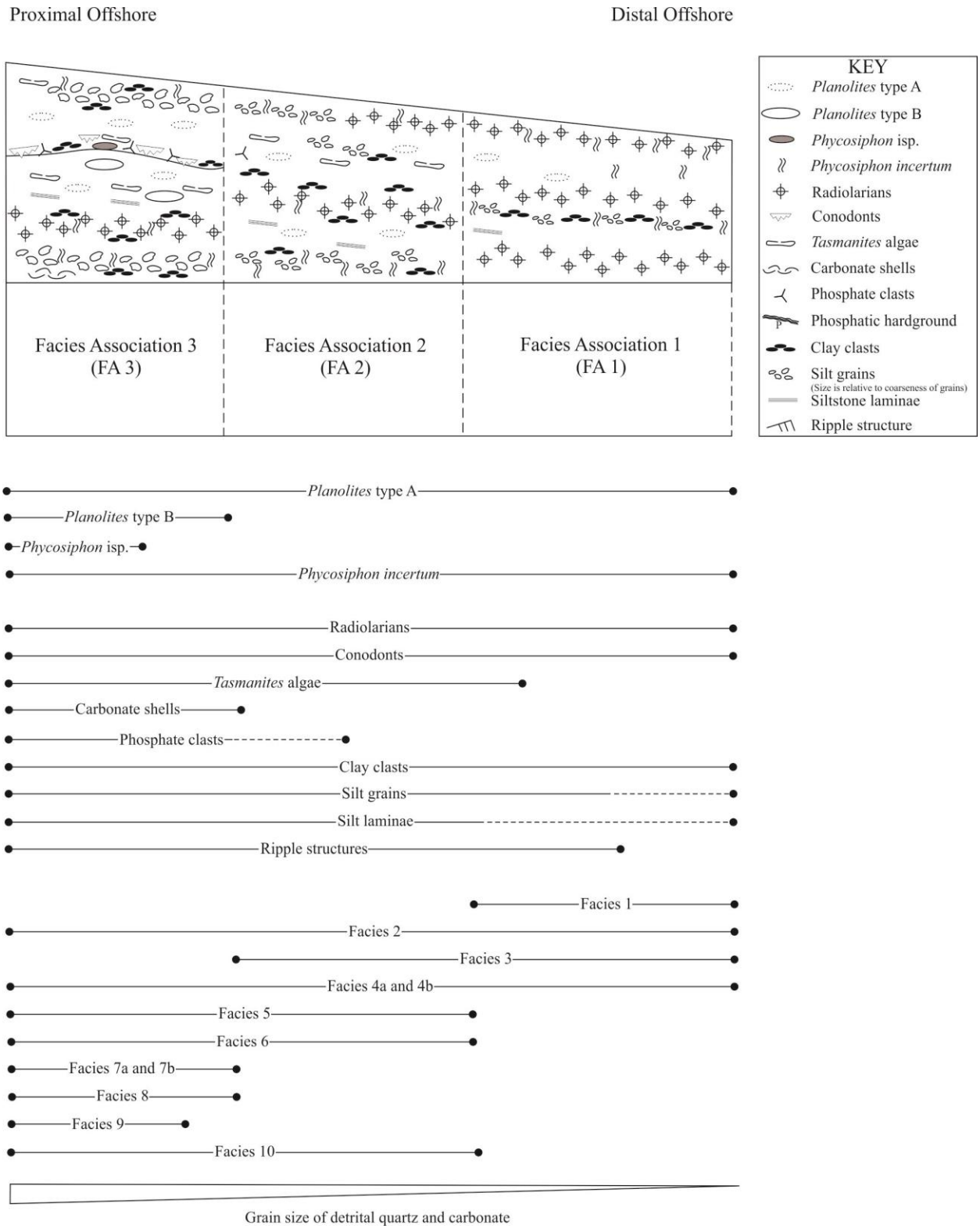

Figure 15B. Depositional model for the lower Bakken shale member in the central and northwestern portions of the study area (Modified from Egenhoff and Fishman, 2013).

7.2 Interpretation of gamma ray (GR) and total organic carbon (TOC) data

The lower Bakken shale member records total GR values between 150-1000 API units throughout the succession. In general, shales have high total gamma ray (GR) values because they are extremely radioactive as clays contain high concentrations of radioactive isotopes of uranium (U), thorium (Th) and potassium (K). Dark, organic-rich shales generally exhibit a stable relationship between extremely high U content and TOC contents (Fertl and Chilingar, 1988; Lüning and Kolonic, 2003). For the lower Bakken shale member, increasing organic matter content towards the uppermost part of the succession in most cores correlates well with increasing GR values (on average 700-900 API units). This correlative relationship between high gamma ray activity, particularly the U peak, with organic shales can be controlled by the rate of sedimentation in the system (Schmoker, 1981; Bohacs et al., 2005). From the base of the lower Bakken shale member into Interval 3, the environment got successively more distal, which would be equivalent to a successively further transport of detrital sediment. It is therefore likely that dilution played a major role in explaining the observed GR patterns in the lower Bakken shale sediments: with increasing distal character of the succession, the amount of detrital sediment delivered to the basin center was reduced, thereby also reducing the dilution of organic matter with sediment. As a result, the amount of organic matter increased towards distal basin areas and so do the API unit values. Nevertheless, this approach means that most likely the production gradient through the basin during lower Bakken times was less pronounced than the sedimentation rate. Even in the center of the basin, organic matter production must have been relatively high in order to explain the observed high TOC values recorded in the sediment.

In contrast to this general trend, though, the Hess Corporation, IM Shorty 0805H-1 core located near the basin margin displays decreasing TOC contents towards the uppermost part of

the succession coupled with decreasing GR values (around 400-600 API units). This core is anomalous in that stratigraphic Interval 2 exhibits the highest GR values in comparison with the other cores in this study that show the highest GR values in Interval 3. Organic productivity rates were high due to the general increase of productivity rates in marginal basin positions (Bohacs et al., 2005). This core is therefore most likely from an anomalous part of the basin that is characterized by a more abundant nutrient supply than other areas, resulting in higher amounts of TOC in the sediment. The coupling of high rates of marine productivity with enhanced organic matter burial that improved preservation in Interval 2 is most likely also responsible for the strong GR response in the Hess Corporation, IM Shorty 0805H-1 core.

Across the study area, portions of stratigraphic Interval 1 that are comprised of heavily bioturbated mudstones with macrofossil debris (FA 3) display a GR profile approximately 200-500 API units lower than most of the succession and also have the lowest TOC values of all four stratigraphic units, with the exception of the Hess Corporation, IM Shorty 0805H-1 core (Appendix 1). This could be the result of (1) benthic organisms consuming more organic matter in FA 3 mudstones than the other FAs and/or (2) higher bottom water oxygen levels in the more proximal mudstones of FA 3 compared to distal FA 1 and FA 2 mudstones, which led to increased disintegration of organic matter during deposition (cf. Borcovsky, 2013). Nevertheless, the relatively strong GR signal of the Hess Corporation, IM Shorty 0805H-1 core also confirms that most likely the production of organic matter was unusually high in this part of the basin and remained so until the end of Interval 2.

8.0 DISCUSSION

8.1 Sea Level Fluctuations

The sequence stratigraphic interpretation of the lower Bakken shale member in this study is based on the overall arrangement of facies and FAs displayed in the four stratigraphic units, Intervals 1-4 (Fig. 16). These intervals can be traced laterally through four regional-scale transects found in Appendices 1-4.

The top of the Upper Three Forks Formation and in places, the Sanish Member, fines upward into the base of the lower Bakken shale member and records the onset of a marine transgression (Smith and Bustin, 2000). The basal contact of the lower Bakken member represents a transgressive surface (LeFever et al., 2011; cf. Van Wagoner et al., 1988) that can appear gradational over 50-350 mm or sharp in places and can be occasionally marked by a phosphate- and fossil-bearing lag deposit. Stratigraphic units, Intervals 1 and 2, represent deposits of the transgressive systems tract (TST). These are displayed as retrogradational stacks of lower Bakken shale facies, indicated by the greater abundance of massive mudstones and siliceous black mudstones (FA 1) in the uppermost parasequences throughout these intervals. However, at the top of Interval 2, a subtle progradational stacking of facies is indicated by the presence of heavily laminated mudstones (FA 2) and thick (>2 mm) siltstone laminae (FA 4) in the uppermost parasequence. Interval 1, along with the lower part of Interval 2, is interpreted to record an initial marine transgression that was followed by a slight overall decrease in sea level during deposition of the topmost parasequence in Interval 2. Since the progradational stacking of facies at the top of Interval 2 is observed in all cores, the slight drop in sea level could potentially represent eustasy. However, this subtle progradational stacking of facies could

possibly reflect minor regional tectonism that occurred in the Williston Basin during deposition of the Bakken Formation, rather than eustasy (Clement, 1985; Gibson, 1995).

In Interval 3, the strata represent early highstand deposits when conditions were the deepest and most tranquil during lower Bakken shale sedimentation, as indicated by the predominance of massive mudstones and siliceous black mudstones (FA 1) and rare high-energy event laminae. Interval 3 is thus interpreted to correspond with maximum flooding of the ramp. The uppermost parasequence in Interval 3, similar to that of Interval 2, records a slight progradational stacking of facies. This is typically represented by proximal laminae of silt-rich facies (FA 4) and/or bioturbated mudstones with macrofossil debris (FA 3) overlying distal massive and siliceous mudstones (FA 1), which probably reflects a minor drop in sea level. Lastly, Interval 4 is interpreted to likely represent late highstand sediments, although prograding facies are only observed in a few cores (e.g. #13098 and 18511, Appendix 2; #2618 and 17723, Appendix 4). Based on this interpretation, Interval 4 would represent late highstand deposits, and indeed some of the cores show it to prograded, with shallower mudstone facies overlying deep shelf Interval 3 mudstones. However, many cores show a fining-upward interpreted to represent a slight deepening of the environment through much of Interval 4. This deepening-upward, which is inconsistent with prograding highstand deposits, can be clarified by incorporating the hitherto non-explained presence of sand-filled clastic dykes penetrating the uppermost parts of the lower shale (Clark and Maldonado, 2011). The sandy fill of these dykes is coarser than any of the over- and underlying units, thereby making it unlikely that these units are a possible source. They exclusively penetrate downwards, therefore suggesting that they must have come from a sand-rich deposit that originally was overlying the lower Bakken shale member, and which is now eroded (Sven Egenhoff, pers. comm., 2014). The most plausible

explanation for the origin of these sandstone dykes is therefore their deposition during a lowstand, most likely the one that followed deposition of the lower Bakken shale member. Following this interpretation, the fining-upward observed in Interval 4 would represent an initial sea-level rise that culminated in another maximum flooding event that is most likely nowhere preserved. Subsequently, relative sea level must have fallen significantly, forming sandy units directly overlying lower Bakken mudstones in the Williston Basin and representing forced regression deposits (cf. Plint and Nummedal, 2000). During earthquakes, the clastic dykes formed, and the sand was injected downward into Interval 4 mudstones. The sandstones must have been eroded again during a subsequent transgression, and only the sand-filled dykes remain as evidence of the former existence of sand-rich lowstand deposits.

On a smaller scale, two different sets of parasequences are observed in the lower Bakken succession: (1) the small-scale, generally coarsening-upwards cycles, and (2) the medium-scale fluctuations, here represented by the intervals. Because of the relief of underlying Three Forks Formation sediments, the amount of small-scale cycles and their thickness varies strongly from core to core, as not all silt-size sediment indicative of a shallowing is delivered to all places in the basin during relative lowstands. Nevertheless, medium-scale trends as represented by Intervals 1 to 4 reflect superimposed long-term cycles that are correlable throughout the basin despite the effect of underlying relief. These intervals show that the Williston Basin was initially deepening during lower Bakken shale member deposition, and this deepening trend includes Intervals 1 to 3 with Interval 3 deep shelf mudstones onlapping onto Interval 2 shallow mudstone deposits. The deepening recorded in the upper part of Interval 4, however, may just represent a short-term transgressive pulse prior to the deposition of sandy lowstand deposits that are now exclusively preserved in the clastic dykes encased in the lower Bakken shales.

From a facies standpoint, the lower Bakken shale is nearly equivalent to the upper Bakken shale (Borcovsky, 2013; Egenhoff and Fishman, 2013), with the exception of *Tasmanites* algae being more frequent in the older unit. However, the internal stacking patterns of the lower Bakken shale are much more complex, with most small-scale cycles not correlable through the basin in the lower member, but all parasequences of the same magnitude are easily traceable through the basin in the upper Bakken member. TOC values are also comparable in both Bakken shales; nevertheless, the stratigraphically older unit shows generally higher TOC values than the upper Bakken shale, with over 20% TOC compared to about 11% TOC. The lower Bakken shale member is thicker than the upper Bakken shale member and likely represents an overall longer time interval. This is also reflected in the number of possible "cycles" in the lower Bakken shale: the lower Bakken shale contains up to twenty-two small-scale parasequences in contrast to only ten in the upper Bakken shale. The medium-scale cycles are only present in the lower Bakken shale, either because (1) the entire upper Bakken shale just represents two of the medium-scale cycles and is therefore subdivided into two distinct intervals (Borcovsky, 2013), or (2) because these cycles did not influence deposition of the upper Bakken shales as much as the lower Bakken shales. However, given the similarities of the two shale units, the former interpretation seems more likely.

The top 4 small-scale parasequences of the upper Bakken shale correlate with the overlying Lodgepole limestone in marginal parts of the basin (Borcovsky, 2013). Because the small-scale cycles are not correlable across the basin for the lower Bakken shale member, it is generally unclear how many of these cycles represent the basinward portion of the middle Bakken siliciclastic ramp. Nevertheless, in a few cores, the uppermost two small-scale parasequences pinch out towards the margin of the basin and are interpreted here to represent a

unit that laterally corresponds to the middle Bakken member. It therefore seems adequate to regard the lower Bakken and the upper Bakken shales as deep shelf equivalents of a shallow-water mixed carbonate-siliciclastic ramp system (Egenhoff et al., 2011) and not an isolated basin containing exclusively black shales without any shallow-water equivalent.

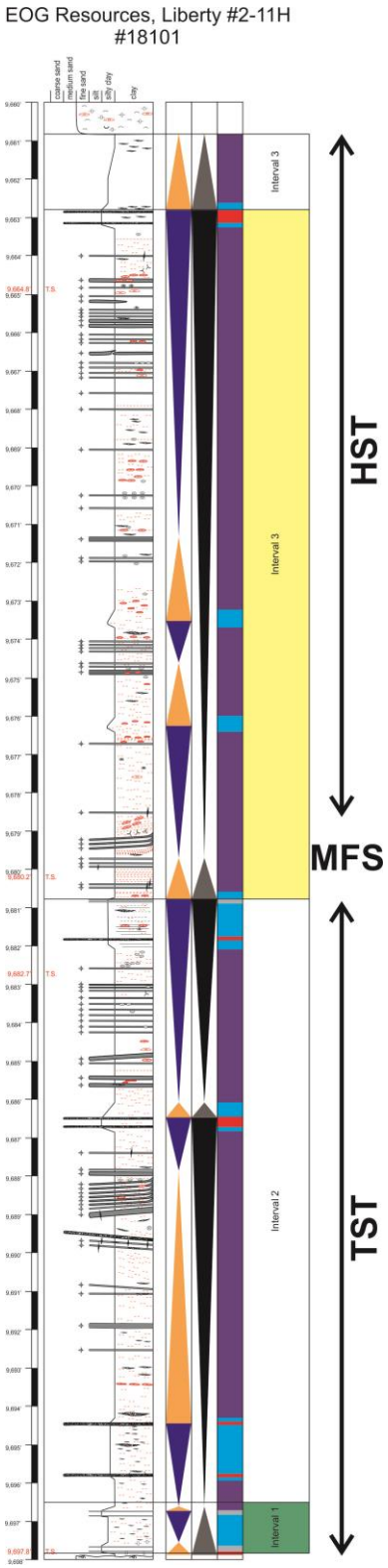

Figure 16. Lithology core log of EOG Resources, Inc. Liberty 2-11H showing parasequences and sequence stratigraphic interpretation. See appendices 1-4 for core log key.

8.2 Geographic Distribution and Preservation of Radiolarite (facies 1) and Radiolaria-bearing Mudstone (facies 2)

Radiolaria-bearing mudstone deposits (facies 2) are most frequent in FA 1 sediments but nevertheless occur in all facies associations. Their commonality among the facies associations is a result of the planktic nature of radiolarians that does not confine them to marked regions of the basin or depth intervals. Thus, the presence of radiolarians alone is not an indicator of a distinct position in the basin, although their occurrence as a mass accumulation does suggest relatively quiet and therefore distal sedimentary conditions in order to be preserved. The preferential accumulation in distal environments is therefore most likely a function of preservation (cf. Bohacs et al., 2005). Relatively low-energy, quiet waters in the distal parts of the basin increase the preservation potential for radiolarians by allowing them to settle from suspension, combined with an infrequency of strong currents that would cause their reworking on the seafloor. Pure radiolarites (facies 1) (70-90% radiolaria microfossils) are therefore most likely to be preserved only in the deep parts of the basin, while in all other lower Bakken settings, sediments containing radiolarians are combined with other constituents from reworking currents such as clay and marine-snow particles (cf. Egenhoff and Fishman, 2013).

8.3 Geographic Distribution of Silt-rich Facies (facies 10)

Silt-rich facies (facies 10) generally occur in the top part of distinct shallowing-upward cycles, but some laminae are also distributed at random through sections of the lower Bakken shale member in the North Dakota portion of the Williston Basin. In addition, the percentage of silt content can vary significantly from core to core in the same stratigraphic interval, even within a few kilometers (Stenehjem HD 27-1 core to Catherine E. Peck #2 core; Appendix 2). These changes in silt content could be explained by the presence of local structures in this basin that influenced preferential deposition of facies within lower Bakken shale strata (Kent and

Christopher, 2007), e.g. paleohighs and -lows, that most likely affected where silt accumulated during lower Bakken shale times (Anna et al., 2011; Kent and Christopher, 2007). Based on the sedimentological model presented in this study, the silt represents laminae caused by storms that brought silt into an environment that is generally characterized by mudstone deposition. These storm surges follow of course gravity, resulting in generally thicker (>7 m) lower Bakken shale member successions in paleolows that have a high silt content with frequent silt-rich laminae (facies 10), and paleohighs (<7 m thick lower Bakken shale succession) with thin sections and little siltstone content. Nevertheless, proximal thin lower Bakken shale sections near the basin margin typically show abundant silt-rich laminae (facies 10) because these areas experienced more frequent high energy events that transported and deposited coarse detritus than regions near the basin depocenter. Based on this model, generally applicable to most of the measured sections, silt distribution is influenced mostly by storms that are generally prone to distribute in tectonically-formed lows influenced by sea-level fluctuations. Distribution of storm deposits is therefore considered to mirror tectonic elements, such as local paleostructures in the basin, as much as it could reflect eustatic or relative sea-level changes.

However, variations in siltstone (facies 10) distribution throughout the Williston Basin could also be a result of sediment source locations during lower Bakken shale member deposition. In northwestern North Dakota, likely sources of sediment were in the north to northeast, as well as one specific point in the south (Fig. 7A-D). This is reflected in cores that display an overall increase in silt content in these areas compared to adjacent cores or to other regions of the study area.

Interestingly, the siltstone (facies 10) distribution in the lower Bakken shale varies significantly from that of the upper Bakken shale. Siltstone (facies 10) variations over a few tens

of kilometers that are frequently observed in the lower Bakken shale member are not as pronounced in the upper Bakken shale. This short-distance change in facies distribution typical for the lower Bakken shale member is most likely caused by a change in relief during the time of deposition. It is likely that the middle Bakken member infilled most, if not all, of the existing paleotopography of the eroded Devonian surface (Martiniuk, 1988; Nicolas and Barchyn, 2008). When the upper Bakken shale was deposited, the basin topography must have been overall smooth (Hayes, 1985), which resulted in easily correlable facies patterns throughout the Williston basin during upper shale member times (cf. Borcovsky, 2013).

8.4 Significance of *Tasmanites* Algae

Tasmanites algae occur in high abundance throughout marginal lower Bakken shale member facies, unlike the upper Bakken shale member of the Bakken Formation, where *Tasmanites* are rare. The frequent occurrence of *Tasmanites* algae in the lower Bakken shale likely reflects consistently high rates of primary productivity in comparison with those during the time of upper Bakken shale deposition. Nitrogen isotope data from Smith and Bustin (1998) imply an abundance of nutrients in the Williston Basin during lower Bakken shale deposition, which was able to support a high rate of marine productivity. The upper Bakken shale member, however, records a transition from light $\delta^{15}N$ values to heavy $\delta^{15}N$ values, indicating a reduction in nutrient supply after the onset of deposition. Seasonally wetter climate conditions during deposition of the lower Bakken shale, in comparison to conditions during upper Bakken shale deposition, could have led to increased runoff and terrestrial supply of nutrients (Ettensohn and Barron, 1981; Smith and Bustin, 1998). Additionally, the climate conditions proposed for the lower Bakken shale member are consistent with the transition from the underlying carbonate Three Forks Formation to the mixed siliciclastic-carbonate system of the overlying middle

Bakken member (Egenhoff et al., 2011). The upper Bakken shale member likely represents a period recording a change from a wetter to drier climate during deposition, as it is overlain by the carbonates of the Lodgepole Formation, which resulted in a decrease in planktonic organisms (cf. Borcovsky, 2013).

8.5 Anoxia

As assumed for most petroleum-relevant shales, deposition of the Bakken Formation (Smith, 1996; Smith and Bustin, 1995, 1998; Sonnenberg, 2011) was envisioned to have taken place under sedimentary conditions that were anoxic during lower shale times and dysoxic during upper shale deposition (Sonnenberg and Pramudito, 2009). A stratified water column (Nordeng, 2009; Webster, 1982) is proposed for this sedimentary system that would have allowed high amounts of organic matter in these shale units to be preserved. However, the ubiquity of *Phycosiphon incertum* fecal strings across all lower Bakken shale member facies, with the exception of locally occurring pure radiolarites (facies 1), indicates that an entirely anoxic environment was improbable. The benthic organisms that produced the *Phycosiphon incertum* fecal strings burrowed at least a few millimeters into the sediment, suggesting that bottom waters were mostly dysoxic during lower Bakken shale deposition, comparable to sedimentation of the upper Bakken shale member (cf. Egenhoff and Fishman, 2013). Low diversity of ichnofossils present throughout the shale succession, however, does reflect stressed conditions in which only specialized organisms could thrive.

9.0 CONCLUSIONS

1. The lower shale member of the Bakken Formation contains eleven facies, ten siliciclastic and one carbonate, that can be grouped into four facies associations (FAs): siliceous black mudstones (FA 1, laminated mudstones (FA 2), bioturbated mudstones with macrofossil debris (FA 3) and silt-rich mudstones (FA 4).
2. The lower Bakken shale member succession can be subdivided into four stratigraphic units, Intervals 1-4, that are differentiated by changes in the predominant facies associations present in each unit. Interval 1 consists of mudstones that are dominated by silt, fossil debris and some macrobioturbation overlain by laminated mudstones intercalated with radiolaria-bearing mudstone laminae of Interval 2. Interval 2 is overlain by Interval 3, which is dominated by massive mudstones containing rare radiolarite and abundant radiolaria-bearing mudstone layers. Interval 4 overlies Interval 3 and represents the topmost portion of the succession that transitions into the middle Bakken member. In places, siltstone and phosphate- and fossil-bearing mudstone laminae occur at the base, but Interval 4 is typically dominated by massive mudstones.
3. The gamma ray (GR) curve of the lower Bakken shale member generally shows 5-6 maxima and 4-5 minima in most cores throughout the entire thickness of the succession. Total GR values typically range between 200 and 900 API units throughout the lower shale. Strong gamma ray responses, GR values reaching 750-900 API units, occur at the base of the succession and within Interval 3, predominantly in massive mudstones. Low GR values between 150 and 400 API units typically occur in Interval 1 in highly bioturbated mudstones.

4. Both bedload and suspension processes are responsible for depositing sediments of the lower Bakken shale member offshore in a distal, low-inclined ramp setting. Ripple structures, clay clasts, lenticular siltstone laminae and lag deposits are indicators of deposition by bedload processes during high energy events, likely storms, while sub-mm clay-rich mudstone laminae of even thickness (facies 3) and radiolarites (facies 1) reflect deposition during quiescent times by suspension settling. The coarsest-grained sediments of all lower Bakken shale FAs were deposited in the most proximal setting and the finest-grained material represents the most distal environment of deposition.
5. Coarsening-upward parasequences in the lower Bakken shale member occur, with predominantly massive mudstones and radiolaria-bearing mudstones (FA 1) at the base that represent minima in depositional energy. The tops of these coarsening-upward parasequences consist of laminated mudstones (FA 2) intercalated with silt-rich mudstones (FA 4) near the basin depocenter that transition into primarily bioturbated mudstones with macrofossil debris (FA 3) and/or silt-rich mudstones (FA 4) around the basin margins. Fining-upward parasequences throughout this succession always display the reverse stacking of facies. As many as thirty parasequences are observed near the basin depocenter, while as few as seven parasequences occur near the basin margin.
6. Lateral correlation of medium-scale parasequences, represented by stratigraphic Intervals 1-4 in this study, provides the basis for a sequence stratigraphic interpretation for the lower Bakken shale member. Interval 1, at the base of the lower shale succession, reflects an initial deepening trend in the Williston Basin that continued through Interval 3, where Interval 3 deep shelf mudstones onlap onto Interval 2 shallow mudstone deposits. The deepening recorded in the upper part of Interval 4, however, may just

represent a short-term transgressive pulse prior to the deposition of sandy lowstand deposits that are now solely preserved in clastic dykes found in the lower Bakken shales.

7. Abundant microscopic bioturbation found in all FAs, e.g. *Phycosiphon incertum* fecal strings, suggests that the depositional environment of the lower Bakken shale member was, at least at times, partially favorable to burrowing organisms. This disagrees with previous studies (Nordeng, 2009; Smith, 1996; Smith and Bustin, 1995, 1998; Sonnenberg, 2011; Webster, 1982) that propose a stratified water column and persistently anoxic conditions in the Williston Basin during this time. It is more likely that conditions during deposition of the lower Bakken shale member were dysoxic to occasionally oxic with rare anoxic conditions only evidenced by radiolarite deposits that lack bioturbation.
8. Differences between the lower Bakken shale and upper Bakken shale members include: (1) abundant *Tasmanites* algae occur in the lower Bakken shale and are relatively rare in the upper Bakken shale, (2) silt-size sediment of the lower Bakken shale is not distributed evenly throughout the basin due to the underlying relief of the Three Forks Formation, whereas the upper Bakken shale was deposited over a leveled topography created during middle Bakken deposition which resulted in easily correlable facies patterns throughout the Williston Basin, (3) small-scale parasequences are easily traceable through the Williston Basin in the upper Bakken shale, while parasequences of the same magnitude are much more complex and not correlable through the basin in the lower Bakken shale, and (4) frequent clay clasts occur throughout the upper Bakken succession while they are less common in the lower Bakken member.

10.0 BIBLIOGRAPHY

Abouelresh, M.O., and Slatt, R.M., 2012, Lithofacies and sequence stratigraphy of the Barnett Shale in east-central Fort Worth Basin, Texas: American Association of Petroleum Geologists (AAPG) Bulletin, v. 96, no. 1, p. 1-22.

Anna, L.O., Pollastro, R., and Gaswirth, S.B., 2011, Williston Basin Province – Stratigraphic and structural framework to a geologic assessment of undiscovered oil and gas resources, chap. 2 *of* U.S. Geological Survey Williston Basin Province Assessment Team, Assessment of undiscovered oil and gas resources of the Williston Basin Province of North Dakota, Montana, and South Dakota (2010): U.S. Geological Survey Digital Data Series 69-W, 17 pp.

Aplin, A.C., and Macquaker, J.H.S., 2011, Mudstone diversity: Origin and implications for source, seal, and reservoir properties in petroleum systems: American Association of Petroleum Geologists (AAPG) Bulletin, v. 95, no. 12, p. 2031-2059.

Blakey, R.C., 2012, Late Devonian – Early Mississippian (360-345 Ma) Paleogeographic Map: Northern Arizona University.

Bohacs, K.M, Neal, J.E., and Grabowski, G.J, Jr., 2002, Sequence stratigraphy in fine-grained rocks: beyond the correlative conformity: 22nd Annual Gulf Coast Section Society for Sedimentary Geology (SEPM) Foundation Bob F. Perkins Research Conference, p. 321-347.

Bohacs, K.M., Grabowski, Jr., G.J., Carroll, A.R., Mankiewicz, P.J., Miskell-Gerhardt, K.J., Schwalbach, J.R., Wegner, M.B., and Simo, J.A., 2005, Production, destruction, dilution, and accommodation – the many paths to source-rock development, *in* Harris, N., ed., The

deposition of organic carbon-rich sediments: Mechanisms, models and consequences: SEPM Special Publication 82, p. 61-101.

Borcovsky, D., 2013, Sedimentology, facies architecture and sequence stratigraphy of a Mississippian age black mudstone succession: the upper member of the Bakken Formation, North Dakota, USA [Unpublished Master's thesis]: Fort Collins, Colorado State University, 110 pp.

Buatois, L.A., and Mángano, M.G., 2011, Ichnology: organism-substrate interactions in space and time: Cambridge University Press, 358 pp.

Chen, Z., Osadetz, K.G., Jiang, C., and Li, M., 2009, Spatial variation of Bakken or Lodgepole oils in the Canadian Williston Basin: American Association of Petroleum Geologists (AAPG) Bulletin, v. 93, p. 829-851.

Clark, W.J., and Maldonado, A.L., 2011, Clastic injectites in the Devonian (Famennian) lower Bakken shale, Williston Basin, North Dakota, *in* Robinson, J.R., LeFever, J.A., and Gaswirth, S.B., eds., The Bakken-Three Forks Petroleum System in the Williston Basin: Rocky Mountain Association of Geologists, p. 127-145.

Clement, J.H., 1985, Cedar Creek: A significant paleotectonic feature of the Williston Basin, *in* Longman, M.W., ed., Williston Basin: Anatomy of a cratonic oil province: Rocky Mountain Association of Geologists, p. 323-336.

Coe, A.L., Bosence, D.W.J., Church, K.D., Flint, S.S., Howell, J.A., and Wilson, R.C.L., 2003, The Sedimentary Record of Sea-Level Change: Cambridge University Press, 287 pp.

Drever, J.I., 1973, The preparation of oriented clay mineral specimens for X-ray diffraction analysis by a filter-membrane peel technique: American Mineralogist, v. 58, no. 5-6, p. 553-554.

Eberl, D.D., 2003, User's guide to RockJock - A program for determining quantitative mineralogy from powder x-ray diffraction data: Open-File Report: 03-78, 55 pp.

Egenhoff, S., Van Dolah, A., Jaffri, A., and Maletz, J., 2011, Facies architecture and sequence stratigraphy of the Middle Bakken Member, North Dakota, *in* Robinson, J.R., LeFever, J.A., and Gaswirth, S.B., eds., The Bakken-Three Forks Petroleum System in the Williston Basin: Rocky Mountain Association of Geologists, p. 27-47.

Egenhoff, S.O., and Fishman, N.S., 2013, Traces in the dark: Sedimentary processes and facies gradients within the Upper Devonian-Lower Mississippian Upper Shale Member of the Bakken Formation, Williston Basin, North Dakota, USA: Journal of Sedimentary Research, v. 83, p. 803-824.

Ettensohn, F.R., and Barron, L.S., 1981, Depositional model for the Devonian-Mississippian black-shale sequence of North America: a tectono-climatic approach: Technical Information Center, Morgantown, U.S. Dept. of Energy, Morgantown Energy Technology Center, DOE/METC/12040-12042.

Fertl, W.H., and Chilingar, G.V., 1988, Total organic carbon determined from well logs: SPE Formation Evaluation, v. 3, no. 2, p. 407-419.

Friedrichs, C.T., and Wright, L.D., 2004, Gravity-driven sediment transport on the continental shelf: Implications for equilibrium profiles near river mouths: Coastal Engineering, v. 51, p. 795-811.

Gerhard, L.C., and Anderson, S.B., 1988, Geology of the Williston Basin (United States Portion), *in* Sloss, L.L., ed., Sedimentary Cover – North America Craton: United States, the Geology of North America, v. D-2: Geological Society of America, Boulder, Colorado, p. 221-241.

Gerhard, L.C., Fischer, D.W., and Anderson, S.B., 1990, Petroleum Geology of the Williston Basin; *in* Leighton, M.W., Kolata, D.R., Oltz, D.F., and Eidel, J.J., eds., Interior cratonic basins: American Association of Petroleum Geologists Memoir 51, p. 507-559.

Gibson, R.I., 1995, Basement tectonics and hydrocarbon production in the Williston Basin: An interpretative overview, *in* Hunter, L.D.V., and Schalla, R.A., eds., 7th International Williston Basin Symposium Guidebook, Montana Geological Society, North Dakota Geological Society, Saskatchewan Geological Society, and Fort Peck Tribes, p. 3-11.

Hammes, U., and Frébourg, G., 2012, Haynesville and Bossier mudrocks: A faces and sequence stratigraphic investigation, East Texas and Louisiana, USA: Marine and Petroleum Geology, v. 31, p. 8-26.

Hansen, W.B., 1991, Geology and horizontal drilling of the Bakken Formation: Billings, Montana Geological Society, 198 pp.

Hayes, M.D., 1985, Conodonts of the Bakken Formation (Devonian and Mississippian), Williston Basin, North Dakota: The Mountain Geologist, v. 22, no. 2, p. 64-77.

Kent, D.M., and Christopher, J.E., 2007, Geological History of the Williston Basin and Sweetgrass Arch, Chapter 27; *in* Mossop, G., and Shetsen, I. comps., Geological Atlas of the Western Canada Sedimentary Basin: accessed at *http://www.ags.gov.ab.ca/publications/ATLAS_WWW/A_CH27/ CH_27_F.shtml.*

Laird, W.M., and Folsom, C.B., Jr., 1956, North Dakota's Nesson Anticline: North Dakota Geological Survey, Report of Investigation, no. 22, 13 pp.

LeFever, J.A., 1991, History of oil production from the Bakken Formation, North Dakota, *in* Hanson, W.B., ed., 1991 guidebook to geology and horizontal drilling of the Bakken Formation: Billings, Montana Geological Society, p. 3-17.

LeFever, J.A., LeFever, R.D., and Nordeng, S.H., 2011, Revised nomenclature for the Bakken Formation (Mississippian-Devonian), North Dakota, *in* Robinson, J.R., LeFever, J.A., and Gaswirth, S.B., eds., The Bakken-Three Forks Petroleum System in the Williston Basin: Rocky Mountain Association of Geologists, p. 11-26.

Lüning, S., and Kolonic, S., 2003, Uranium spectral gamma-ray response as a proxy for organic richness in black shales: Applicability and limitations: Journal of Petroleum Geology, v. 26, no. 2, p. 153-174.

Macquaker, J.H.S., and Gawthorpe, R.L., 1993, Mudstone lithofacies in the Kimmeridge Clay Formation, Wessex Basin, Southern England: Implications for the origin and controls of the distribution of mudstones: Journal of Sedimentary Petrology, v. 63, no. 6, p. 1129-1143.

Macquaker, J.H.S., and Taylor, K.G., 1996, A sequence-stratigraphic interpretation of a mudstone-dominated succession: the Lower Jurassic Cleveland Ironstone Formation, UK: Journal of the Geological Society, London, v. 153, p. 759-770.

Macquaker, J.H.S., Gawthorpe, R.L., Taylor, K.G., and Oates, M.J., 1998, Heterogeneity, stacking patterns and sequence stratigraphic interpretation in distal mudstone successions; examples from the Kimmeridge Clay Formation, U.K., *in* Schieber, J., Zimmerle, W., Sethi, P.S., eds., Shales and Mudstones: I. Basin Studies, Sedimentology, and Paleontology. Schweizerbart, Stuttgart, Germany, p. 163-186.

Macquaker, J.H.S., and Howell, J.K., 1999, Small-scale (<5.0 m) vertical heterogeneity in mudstones: implications for high-resolution stratigraphy in siliciclastic mudstone successions: Journal of the Geological Society, London, v. 156, p. 105-112.

Macquaker, J.H.S., and Jones, C.R., 2002, A sequence-stratigraphic study of mudstone heterogeneity: A combined petrographic wireline log investigation of Upper Jurassic mudstones from the North Sea (U.K.), *in* Lovell, M., and Parkinson, N., eds., Geological applications of well logs: American Association of Petroleum Geologists (AAPG) Methods in Exploration, no. 13, p. 123-141.

Macquaker, J.H.S., and Adams, A.E., 2003, Maximizing information from fine-grained sedimentary rocks; an inclusive nomenclature for mudstones: Journal of Sedimentary Research, v. 73, no. 5, p. 735-744.

Macquaker, J.H.S., Taylor, K.G., and Gawthorpe, R.L., 2007, High-resolution facies analyses of mudstones: Implications for paleoenvironmental and sequence stratigraphic interpretations of offshore ancient mud-dominated successions: Journal of Sedimentary Research, v. 77, p. 324-339.

Macquaker, J.H.S., Bentley, S.J., and Bohacs, K.M., 2010, Wave-enhanced sediment-gravity flows and mud dispersal across continental shelves: Reappraising sediment transport processes operating in ancient mudstone successions: Geology, v. 38, no. 10, p. 947-950.

Martiniuk, C.D., 1988, Regional geology and petroleum potential of the Bakken Formation, southwestern Manitoba: Manitoba Energy and Mines, Petroleum Branch, Petroleum Open File Report POF8-88, 34 pp.

McCarthy, K., Rojas, K., Niemann, M., Palmowski, D., Peters, K., Stankiewicz, A., 2011, Basic petroleum geochemistry for source rock evaluation: Schlumberger *Oilfield Review* Summer 2011: 23, no. 2, 12 pp.

Meissner, F. F., 1978, Petroleum Geology of the Bakken Formation Williston Basin, North Dakota and Montana, *in* The economic geology of the Williston Basin: The Montana Geological Society 24th Annual Conference, 1978 Williston Basin Symposium, p. 207-227.

Meissner, F.F., and Banks, R.B., 2000, Computer simulation of hydrocarbon generation, migration and accumulation under hydrodynamic conditions: Examples from the Williston and San Juan Basins, USA: American Association of Petroleum Geologists (AAPG) Bulletin, v. 84, no. 9, p. 1464.

Montgomery, S.L., 1997, Ordovician Red River "B": horizontal oil play in southern Williston Basin: American Association of Petroleum Geologists (AAPG) Bulletin, v. 81, p. 519-532.

Murphy, E.C., Nordeng, S.H., Juenker, B.J., and Hoganson, J.W., 2009, North Dakota Stratigraphic Column: North Dakota Geological Survey, Miscellaneous Series 91, 1 pp.

Nicolas, M.P.B., and Barchyn, D., 2008, Williston Basin project (Targeted Geoscience Initiative II): Summary report on Paleozoic stratigraphy, mapping and hydrocarbon assessment, southwestern Manitoba: Manitoba Science, Technology, Energy and Mines, Manitoba Geological Survey Geoscientific Paper GP2008-2, 21 pp.

Nordeng, S.H., 2009, The Bakken petroleum system: an example of a continuous petroleum accumulation: North Dakota Geological Survey, DMR Newsletter 36(1), p. 21-24.

Pitman, J.K., Price, L.C., and LeFever, J.A., 2001, Diagenesis and fracture development in the Bakken Formation, Williston Basin: Implications for reservoir quality in the middle member: U.S. Geological Survey, U.S. Geological Survey Professional Paper 1653, Denver, Colorado, 19 pp.

Plint, A.G., and Nummedal, D., 2000, The falling stage systems tract: Recognition and importance in sequence stratigraphic analysis, *in* Hunt, D., and Gawthorpe, R.L., eds., Sedimentary response to forced regression: Geological Society of London Special Publication, v. 172, p. 1-17.

Pollastro, R.M., 1982, A recommended procedure for the preparation of oriented clay-mineral specimens for X-ray diffraction analysis; modifications to Drever's filter-membrane peel technique: United States Geological Survey Open-File Report: 82-71, 24 pp.

Pollastro, R.M., Cook, T.A., Roberts, L.N.R., Schenk, C.J., Lewan, M.D., Anna, L.O., Gaswirth, S.B., Lillis, P.G., Klett, T.R., and Charpentier, R.R., 2008, Assessment of undiscovered oil resources in the Devonian-Mississippian Bakken Formation, Williston Basin Province, Montana and North Dakota, 2008: U.S. Geological Survey Fact Sheet 2008–3021, 2 pp.

Pollastro, R.M., Roberts, L.N.R., and Cook, T.A., 2011, Geologic Assessment of Technically Recoverable Oil in the Devonian and Mississippian Bakken Formation, Chapter 5, *in* U.S. Geological Survey Williston Basin Province Assessment Team, Assessment of undiscovered oil and gas resources of the Williston Basin Province of North Dakota, Montana and South Dakota: U.S. Geological Survey Digital Data Series, DDS-69-W, 7 chaps., 34 pp.

Schieber, J., 1996, Early diagenetic silica in algal cysts and spores: A source of sand in black shales?: Journal of Sedimentary Research, v. 66, p. 175-183.

Schieber, J., 1998a, Developing a sequence stratigraphic framework for the Late Devonian Chattanooga Shale of the southeastern U.S.A.: relevance for the Bakken Shale, *in* Christopher, J.E., Gilboy, C.F., Paterson, D.F. and Bend, S.L., eds., Eighth International Williston Basin Symposium, Saskatchewan Geological Society Special Publication, no. 13, p. 58-68.

Schieber, J., 1998b, Sedimentary features indicating erosion, condensation, and hiatuses in the Chattanooga Shale of Central Tennessee: Relevance for sedimentary and stratigraphic evolution, *in* Schieber, J., Zimmerle, W., and Sethi, P., eds., Shales and Mudstones, volume I: volume I: Stuttgart, E. Schweizerbart'sche Verlagsbuchhandlung, p. 187-215.

Schieber, J., 2003, Simple gifts and buried treasures – Implications of finding bioturbation and erosion surfaces in black shales: The Sedimentary Record, v. 1, p. 4-8.

Schieber, J., and Zimmerle, W., 1998, Petrography of shales: A survey of techniques, *in* Schieber, J., Zimmerle, W., and Sethi, P., eds., Shales and Mudstones, volume II: Stuttgart, E. Schweizerbart'sche Verlagsbuchhandlung, p. 3-12.

Schieber, J., and Southard, J., 2009, Bedload transport of mud by floccule ripples: Direct observation of ripple migration processes and their implications: Geology, v. 37, no. 6, p. 483-486.

Schieber, J., Southard, J., and Schimmelmann, A., 2010, Lenticular shale fabrics resulting from intermittent erosion of water-rich muds: Interpreting the rock record in the light of recent flume experiments: Journal of Sedimentary Research, v. 80, p. 119-128.

Schmoker, J.W., 1981, Determination of organic-matter content of Appalachian Devonian shales from gamma-ray logs: American Association of Petroleum Geologists (AAPG) Bulletin, v. 65, no. 7, p. 1258-1298.

Schmoker, J.W., and Hester, T.C., 1983, Organic Carbon in Bakken Formation, United States Portion of Williston Basin: American Association of Petroleum Geologists (AAPG) Bulletin, v. 67, no. 12, p. 2165-2174.

Smith, M.G., 1996, The Bakken Formation (Late Devonian-Early Mississippian): A black shale source rock in the Williston Basin [Doctor of Philosophy Dissertation]: Vancouver, The University of British Columbia, 807 pp.

Smith, M.G., and Bustin, M.R., 1995, Sedimentology of the Late Devonian and Early Mississippian Bakken Formation, Williston Basin: 1995 guidebook for the 7th International Williston Basin Symposium, v. 12, p. 103-114.

Smith, M.G., and Bustin, M.R., 1998, Production and preservation of organic matter during deposition of the Bakken Formation (Late Devonian and Early Mississippian), Williston Basin: Palaeo, v. 142, p. 185-200.

Smith, M.B., and Bustin, M.R., 2000, Late Devonian and Early Mississippian Bakken and Exshaw Black Shale Source Rocks, Western Canada Sedimentary Basin: A sequence stratigraphic interpretation: American Association of Petroleum Geologists (AAPG) Bulletin, v. 894, no. 7, p. 940-960.

Sonnenberg, S.A., 2011, TOC and pyrolysis data for the Bakken shales, Williston Basin, North Dakota and Montana, *in* Robinson, J.W., LeFever, J.A., and Gaswirth, S.B., eds., The Bakken-Three Forks Petroleum System in the Williston Basin, Denver, Colorado: Rocky Mountain Association of Geologists, p. 308-331.

Sonnenberg, S.A., and Pramudito, A., 2009, Petroleum geology of the giant Elm Coulee field, Williston Basin: American Association of Petroleum Geologists (AAPG) Bulletin, v. 93, no. 9, p. 1127-1153.

Soukup, D.A., Buck, B.J., and Harris, W., 2008, Preparing soils for mineralogical analysis, *in* Ulery, A.L., and Drees, L.R., eds., Methods of soil analysis, Part 5, Mineralogical Methods: SSSA Book Serv. 5, SSSA, Madison, WI, p. 13-31.

Tappan, H., 1980, The Paleobiology of Plant Protists: San Francisco, W.H. Freeman and Co., 1028 pp.

Tyson, R.V., and Pearson, T.H., 1991, Modern and ancient continental shelf anoxia: An overview: Geological Society, London, Special Publications, v. 58, p. 1-24.

Van Wagoner, J.C., Posamentier, H.W., Mitchum, R.M.J., Vail, P.R., Sarg, J.F., Loutit, T.S., and Hardenbol, J., 1988, An overview of the fundamentals of sequence stratigraphy and key definitions. Sea-Level Changes: An Integrated Approach: SEPM, Special Publication, v. 42, p. 39-45.

Webster, R.W., 1982, Analysis of petroleum source rocks and stratigraphy of the Bakken Formation, *in* Woodward, J., Meissner, F.F., and Clayton, J.L., eds., Hydrocarbon source rocks of the greater Rocky Mountain region, Denver, Colorado: Rocky Mountain Association of Geologists, p. 57-82.

Woodrow, D.L., Fletcher, F.W., and Ahrnsbrak, W.F., 1973, Paleogeography and paleoclimate of the depositional sites of the Devonian Catskill and the Old Red Facies: Geological Society of America (GSA) Bulletin 84, p. 3051-3064.

11.0 APPENDICES

Appendix 1: Northern West-East transect through the North Dakota portion of the lower Bakken shale member, Williston Basin

Appendix 2: Southern West-East transect through the North Dakota portion of the lower Bakken shale member, Williston Basin

Appendix 3: North-South transect through the Western North Dakota portion of the lower Bakken shale member, Williston Basin

Appendix 4: North-South transect through the Eastern North Dakota portion of the lower Bakken shale member, Williston Basin

Appendix 5: Thin section index

Original Operator	Original Well Name	Well ID No.	Thin Section No. (Depth (ft))	Facies Association	Facies	Silt Min. (%)		Total Silt (%)	Dominant Grain-size (Normalized to 100%)			Clay Clasts (%)	*Tasmanites (%)*
						Detrital Qtz	Carbonate		Fine silt (%)	Medium Silt (%)	Coarse Silt (%)		
Amerada Hess Corp.	Anderson Smith 1-26H	16083	9776.9	2	3	27	7	34	90	8	2	10	0
Amerada Hess Corp.	Anderson Smith 1-26H	16083	9791.2	1	4a	21	2	23	65	30	5	5	0
Amerada Hess Corp.	H. Bakken 12-07H	16565	9699.5	1	3	THIN SECTION TOO THICK			-	-	-	0	5
Amerada Hess Corp.	IM Shorty 0805 H-1	17272	7603.9 (lower)	2	2	-	-	0	-	-	-	0	3
Amerada Hess Corp.	IM Shorty 0805 H-2	17272	7603.9 (upper)	2	4a	16	0	16	45	54	1	0	<1
Amerada Hess Corp.	RS-Nelson 1423 H-1	16824	9257.5 (lower)	1	3	15	1	16	58	42	0	3	5
Amerada Hess Corp.	RS-Nelson 1423 H-2	16824	9257.5 (middle)	3	7a	10	8	18	54	44	2	2	5
Amerada Hess Corp.	RS-Nelson 1423 H-3	16824	9257.5 (upper)	1	5	15	1	16	58	42	0	3	10
Amerada Hess Corp.	RS-Nelson 1423 H-1	16824	9258.3	1	5	11	3	14	50	45	5	7	50
Amerada Hess Corp.	RS-State 3603 H-1	17071	8815.3	2	4a	14	0	14	90	6	4	10	2
Amerada Hess Corp.	State of ND 1-11H	16160	9528.6 (lower)	3	7a	14	2	16	85	10	5	0	2
Amerada Hess Corp.	State of ND 1-11H	16160	9528.6 (upper)	3	4a	11	1	12	83	13	4	0	2
Brigham Oil & Gas	Olson 10-15 1-H	17513	10655.75 (lower)	2	3	22	1	23	75	20	5	0	2
Brigham Oil & Gas	Olson 10-15 1-H	17513	10655.75 (upper)	3	7a	26	0	26	80	18	2	0	<1
Brigham Oil & Gas	Olson 10-15 1-H	17513	10658.9	2	4a	10	0	10	35	65	0	0	3
Brigham Oil & Gas	Olson 10-15 1-H	17513	10667.6 (lower)	2	4a	30	2	32	67	27	6	0	0
Brigham Oil & Gas	Olson 10-15 1-H	17513	10667.6 (upper)	2	3	17	1	18	70	30	0	0	0
Brigham Oil & Gas	Olson 10-15 1-H	17513	10678.2	3	9	11	2	13	75	20	5	0	0
Brigham Oil & Gas	Olson 10-15 1-H	17513	10679.4	3	9	32	6	38	75	22	3	0	0
EOG Resources, Inc.	Liberty 2-11H	18101	9664.8 (lower)	1	3	3	1	4	80	15	5	25	6
EOG Resources, Inc.	Liberty 2-11H	18101	9664.8 (upper)	1	2	8	1	9	55	35	10	10	1
EOG Resources, Inc.	Liberty 2-11H	18101	9680.2	1	4a	11	9	20	60	38	2	0	7
EOG Resources, Inc.	Liberty 2-11H	18101	9682.7	1	3	21	2	23	50	45	5	5	8
EOG Resources, Inc.	Liberty 2-11H	18101	9697.8	3	9	20	2	22	70	25	5	12	1
EOG Resources, Inc.	McAlmond 1-05H	16862	8853.3	1	2	-	-	0	-	-	-	0	1
EOG Resources, Inc.	McAlmond 1-05H	16862	8864.8	1	2	15	2	17	65	35	0	0	12
EOG Resources, Inc.	McAlmond 1-05H	16862	8866.9	1	5	15	1	16	75	20	5	12	10
EOG Resources, Inc.	McAlmond 1-05H	16862	8869.5 (lower)	3	7b	8	2	10	80	10	10	25	8
EOG Resources, Inc.	McAlmond 1-05H	16862	8869.5 (upper)	1	4b	12	3	15	65	35	0	15	5
EOG Resources, Inc.	Van Hook 1-13H	16997	9506.1	2	3	16	1	17	60	25	15	3	2
EOG Resources, Inc.	Van Hook 1-13H	16997	9522.3	1	5	19	4	23	70	25	5	0	10
EOG Resources, Inc.	Van Hook 1-13H	16997	9525.5	1	-	-	-	0	-	-	-	-	-
EOG Resources, Inc.	Van Hook 1-13H	16997	9527.4	4	7a	11	1	12	65	25	10	6	5
EOG Resources, Inc.	Van Hook 1-13H	16997	9530.8 (lower)	3	7b	11	1	12	70	25	5	10	3
EOG Resources, Inc.	Van Hook 1-13H	16997	9530.8 (upper)	2	3	18	1	19	80	12	8	0	8
EOG Resources, Inc.	Van Hook 1-13H	16997	9536.3	3	7b	17	1	18	64	32	4	15	7
EOG Resources, Inc.	Van Hook 1-13H	16997	9538.1 (lower)	4	7b	8	1	9	60	10	30	20	5
EOG Resources, Inc.	Van Hook 1-13H	16997	9538.1 (upper)	1	3	6	1	7	75	20	5	0	2

Headington Oil Co.	Nesson State 42X-36	17015	10404.5	4	4a	19	5	24	62	31	7	1	0
Headington Oil Co.	Nesson State 42X-37	17015	10409.5	1	3	10	2	12	76	21	3	1	<1
Headington Oil Co.	Nesson State 42X-38	17015	10426.5	3	9	34	4	38	73	25	2	0	0
Newfield Production Co.	Chanel 1-33H	18226	10661.9 (lower)	1	4a	8	2	10	70	25	5	0	0
Newfield Production Co.	Chanel 1-33H	18226	10661.9 (middle)	1	2	6	1	7	70	30	0	0	0
Newfield Production Co.	Chanel 1-33H	18226	10661.9 (upper)	1	4a	7	1	8	70	28	2	5	0
Newfield Production Co.	Jorgenson 1-15H	17086	11029.5	1	3	19	3	22	84	16	0	5	0
Newfield Production Co.	Jorgenson 1-15H	17086	11034.6 (lower)	3	11	6	1	7	85	12	3	0	0
Newfield Production Co.	Jorgenson 1-15H	17086	11034.6 (middle)	1	3	13	2	15	55	42	3	0	0
Newfield Production Co.	Jorgenson 1-15H	17086	11034.6 (upper)	1	3	6	5	11	70	20	10	0	0
Newfield Production Co.	Sergeant Major 1-21H	18086	11100.75	N/A	N/A	17	1	18	70	10	20	0	0
Newfield Production Co.	Sergeant Major 1-21H	18086	11110.85	1	3	18	2	20	67	28	5	0	0
Newfield Production Co.	Sergeant Major 1-21H	18086	11114.6	3	8	22	10	32	40	35	25	0	0
Newfield Production Co.	Sergeant Major 1-21H	18086	11120.3	3	9	29	6	35	12	47	41	0	0
Newfield Production Co.	Sergeant Major 1-21H	18086	11121.7	1	3	16	1	17	75	20	5	0	0
Newfield Production Co.	Sergeant Major 1-21H	18086	11138.2	3	9	28	2	30	50	40	10	0	0
North Plains Energy, LLC	Scanlan 3-5H	18770	11073.5	1	2	THIN SECTION TOO THICK			-	-	-	0	0
North Plains Energy, LLC	Scanlan 3-5H	18770	11074	4	4a	20	10	30	60	25	15	0	0
North Plains Energy, LLC	Scanlan 3-5H	18770	11075.5 (lower)	1	-	THIN SECTION TOO THICK			-	-	-	-	-
North Plains Energy, LLC	Scanlan 3-5H	18770	11075.5 (upper)	1	3	30	10	40	55	30	15	0	0
North Plains Energy, LLC	Scanlan 3-5H	18770	11084.5	2	3	16	3	19	82	16	2	5	0
Pogo Producing Co., LLC	Pegasus 2-17H	16405	10182.4	1	3	16	4	20	75	24	1	5	0
Whiting Oil & Gas Corp.	Braaflat 11-11H	17023	9941.7	1	3	15	1	16	85	15	0	15	7
Whiting Oil & Gas Corp.	Braaflat 11-11H	17023	9948.2 (lower)	3	7a	12	2	14	50	40	10	2	70
Whiting Oil & Gas Corp.	Braaflat 11-11H	17023	9948.2 (upper)	2	3	16	1	17	70	25	5	0	8
XTO Energy, Inc.	Miller 34X-9	17723	9508.7	1	5	15	1	16	75	25	0	15	12

Appendix 6: Total organic carbon and Rock-Eval pyrolysis data

Weatherford LABORATORIES

TOTAL ORGANIC CARBON, PROGRAMMED PYROLYSIS DATA

Company : CSU **Project No :** BH-68379 / BH-68379

Client ID	Well Name	Depth () Top	Sample Type	Sample Prep	*	Facies Association	Leco TOC	RE S1	RE S2	RE S3	Tmax (°C)	**	Ro, %	HI	OI	S2/S3	S1/TOC* 100	PI	Notes Checks	Notes Pyrogram	LAB ID
	Well 16160	9495.2	Powder Rock	NOPR		1	15.10														3.403E+09
	Well 16160	9502.3	Powder Rock	NOPR		1	9.49												TOC		3.403E+09
	Well 16160	9509.8	Powder Rock	NOPR		2	10.80														3.403E+09
	Well 16160	9511.8	Powder Rock	NOPR		1	12.60														3.403E+09
	Well 16160	9516	Powder Rock	NOPR		1	11.70														3.403E+09
	Well 16160	9519.1	Powder Rock	NOPR		1	14.40	7.49	52.64	0.67	441			366	5	78.6	52	0.12	RE	n1ts2sh	3.403E+09
	Well 16160	9521.5	Powder Rock	NOPR		1	13.10														3.403E+09
	Well 16160	9523.8	Powder Rock	NOPR		1	12.70												TOC		3.403E+09
	Well 16160	9528.3	Powder Rock	NOPR		1	9.51														3.403E+09
	Well 16160	9532.4	Powder Rock	NOPR		1	1.43												TOC		3.403E+09
	Well 16160	9533.7	Powder Rock	NOPR		1	1.16												TOC		3.403E+09
	Well 17015	10392.2	Powder Rock	NOPR		1	14.65												TOC		3.403E+09
	Well 17015	10394.8	Powder Rock	NOPR		1	12.50														3.403E+09
	Well 17015	10395.5	Powder Rock	NOPR		1	11.20														3.403E+09
	Well 17015	10400.25	Powder Rock	NOPR		1	12.60														3.403E+09
	Well 17015	10401.5	Powder Rock	NOPR		1	12.60	6.18	28.65	0.58	447			227	5	49.4	49	0.18	RE	n1ts2sh;hts2sh	3.403E+09
	Well 17015	10409.2	Powder Rock	NOPR		1	10.30														3.403E+09
	Well 17015	10415.4	Powder Rock	NOPR		1	9.16														3.403E+09
	Well 17015	10418.1	Powder Rock	NOPR		2	8.48												TOC		3.403E+09
	Well 17015	10421.5	Powder Rock	NOPR		1	9.63														3.403E+09
	Well 17015	10426.9	Powder Rock	NOPR		1	8.29														3.403E+09
	Well 17015	10431	Powder Rock	NOPR		1	6.70														3.403E+09
	Well 17015	10435.6	Powder Rock	NOPR		1	3.33												TOC		3.403E+09
	Well 17023	9932.4	Powder Rock	NOPR		1	16.80												TOC		3.403E+09
	Well 17023	9933.8	Powder Rock	NOPR		1	18.50														3.403E+09
	Well 17023	9935.8	Powder Rock	NOPR		1	15.90														3.403E+09
	Well 17023	9941.7	Powder Rock	NOPR		1	8.94	7.80	46.72	0.73	435			523	8	64.0	87	0.14	RE	n1ts2sh	3.403E+09
	Well 17023	9947.9	Powder Rock	NOPR		2	13.70														3.403E+09
	Well 17023	9951.5	Powder Rock	NOPR		1	10.70														3.403E+09
	Well 17023	9953.35	Powder Rock	NOPR		1	10.90														3.403E+09
	Well 17023	9955.5	Powder Rock	NOPR		1	10.75												TOC		3.403E+09
	Well 17023	9958.7	Powder Rock	NOPR		1	18.00														3.403E+09

Weatherford LABORATORIES

TOTAL ORGANIC CARBON, PROGRAMMED PYROLYSIS DATA

Company : CSU **Project No :** BH-68379 / BH-68379

Client ID	Well Name	Depth () Top	Sample Type	Sample Prep	*	Facies Association	Leco TOC	RE S1	RE S2	RE S3	Tmax (°C)	**	Ro, %	HI	OI	S2/S3	S1/TOC* 100	PI	Notes Checks	Notes Pyrogram	LAB ID
	Well 17023	9960.8	Powder Rock	NOPR		1	20.40														3.403E+09
	Well 17023	9962	Powder Rock	NOPR		1	19.90														3.403E+09
	Well 17023	9966.5	Powder Rock	NOPR		1	3.07														3.403E+09
	Well 17023	9967.5	Powder Rock	NOPR		1	2.54												TOC		3.403E+09
	Well 17272	7595.7	Powder Rock	NOPR		1	3.16														3.403E+09
	Well 17272	7596.8	Powder Rock	NOPR		1	2.99												TOC		3.403E+09
	Well 17272	7599.8	Powder Rock	NOPR		2	5.25	2.87	7.56	0.53	424			144	10	14.3	55	0.27	RE	n:lts2sh	3.403E+09
	Well 17272	7601.4	Powder Rock	NOPR		1	16.70														3.403E+09
	Well 17272	7603	Powder Rock	NOPR		1	19.20														3.403E+09
	Well 17272	7606	Powder Rock	NOPR		1	16.10														3.403E+09

Notes:

"-1" – not measured or invalid value for Tmax
TOC - Total Organic Carbon, wt. %
S1 - volatile hydrocarbon (HC) content, mg HC/ g rock
S2 - remaining HC generative potential, mg HC/ g rock
S3 - carbon dioxide content, mg CO2 / g rock

* - comments regarding contamination
** - low S2. Tmax is unreliable
Meas. %Ro - measured vitrinite reflectance
HI - Hydrogen index = S2 x 100 / TOC, mg HC/ g TOC
OI - Oxygen Index = S3 x 100 / TOC, mg CO2/ g TOC
PI - Production Index = S1 / (S1+S2)

Pyrogram:

f - flat S2 peak
n - normal
ltS2sh - low temperature S2 shoulder
htS2sh - high temperature S2 shoulder
ltS2p - low temperature S2 peak
htS2p - high temperature S2 peak

LECO – TOC on Leco Instrument
RE - Programmed pyrolysis or TOC on Rock-Eval instrument
SRA – Programmed pyrolysis by SRA Instrument
EXT - Extracted Rock
NOPR - Normal Preparation

Weatherford LABORATORIES

GEOCHEMICAL LOGS

Company: CSU | Project #: BH-68379 / BH-68379

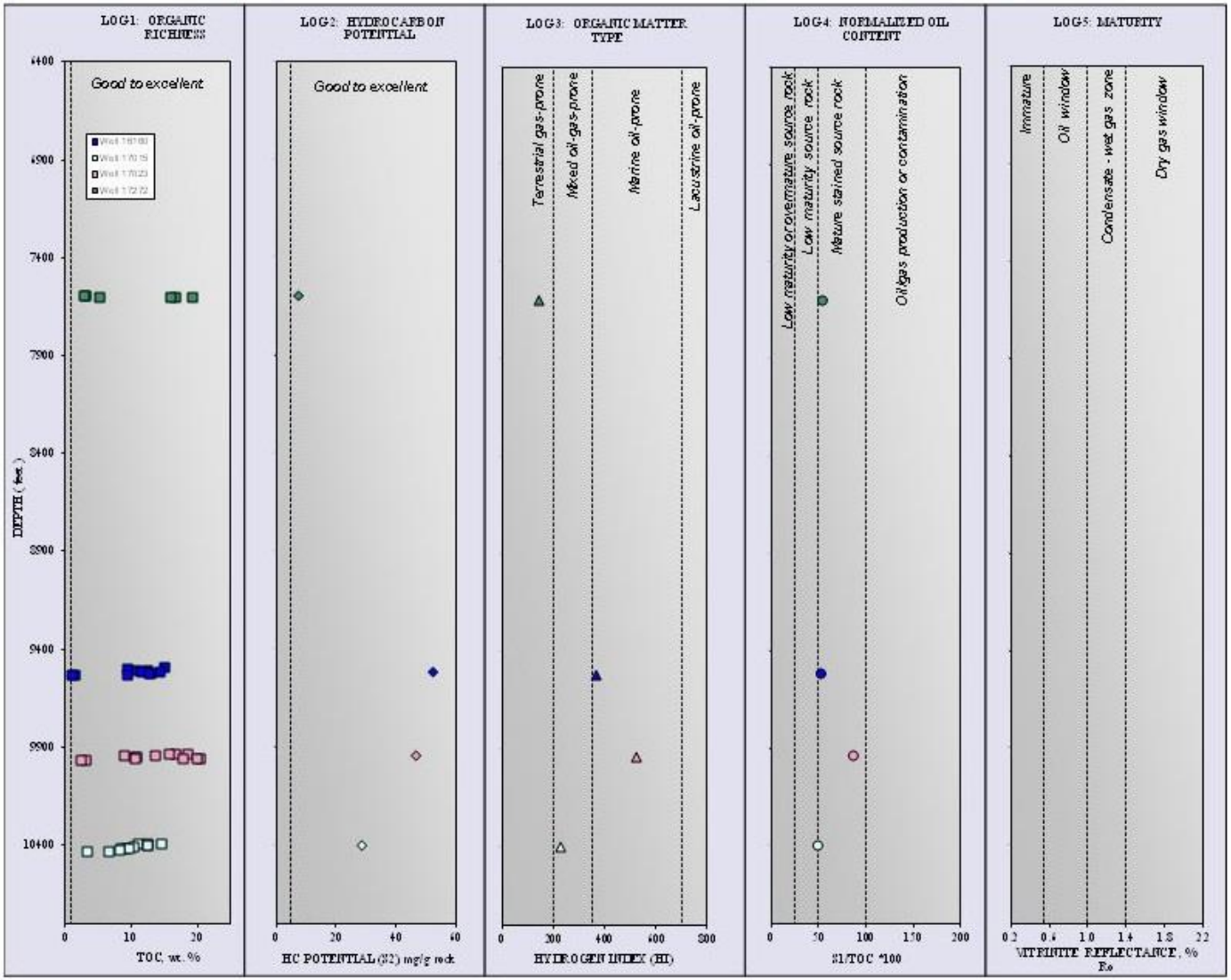

Appendix 7: X-ray diffraction (XRD) data

Well #17015 Headington Oil Company, Nesson State 42X-36															
Sample Name	Depth	Facies Association	NON-CLAYS	Quartz	Kspar (Sanidine)	Plagioclase (Albite)	**Total Feldspar**	Dolomite	Pyrite	**Total Non-Clays**	CLAYS	Illite (1Md)	Illite (2M)	**Total Clays**	**TOTAL**
17015@10393.1	10393.1	2/4		35.0	17.0	-	17.0	3.0	4.0	59.0		9.0	32.0	41.0	100.0
17015@10404.5	10404.5	2/4		39.0	18.0	-	18.0	5.1	6.7	68.8		5.3	26.1	31.4	100.2
17015@10419.8	10419.8	2		44.2	16.5	-	16.5	4.5	8.0	73.2		4.6	22.1	26.7	99.9
17015@10422.3	10422.3	2		40.8	17.6	-	17.6	4.9	7.4	70.7		4.8	24.5	29.3	100.0
17015@10427.35	10427.35	2		29.4	21.1	-	21.1	4.9	5.2	60.6		9.1	30.3	39.4	100.0
17015@10433.2	10433.2	2/4		41.2	18.0	-	18.0	2.6	14.2	76.0		4.6	19.4	24.0	100.0

Well #17272 Hess Corporation, IM Shorty 0805H-1															
Sample Name	Depth	Facies Association	NON-CLAYS	Quartz	Kspar (Sanidine)	Plagioclase (Albite)	**Total Feldspar**	Dolomite	Pyrite	**Total Non-Clays**	CLAYS	Illite (1Md)	Illite (2M)	**Total Clays**	**TOTAL**
17272@7593.8	7593.8	2/4		26.3	12.6	4.6	17.2	3.7	2.3	49.5		18.2	32.2	50.4	99.9
17272@7597.3	7597.3	2		27.1	15.3	5.0	20.3	-	3.4	50.8		13.9	35.3	49.2	100.0
17272@7599.9	7599.9	2/4		35.6	13.4	3.2	16.6	3.8	1.6	57.6		11.5	30.9	42.4	100.0
17272@7603.7	7603.7	2		35.9	15.1	5.4	20.5	-	2.8	59.2		7.1	33.7	40.8	100.0